UCSF
UC San Francisco Electronic Theses and Dissertations

Title
Dynamic behaviors of progenitors and neurons in the gyrencephalic cortex

Permalink
https://escholarship.org/uc/item/1h33b7hq

Author
Gertz, Caitlyn Cody

Publication Date
2015

Supplemental Material
https://escholarship.org/uc/item/1h33b7hq#supplemental

Peer reviewed|Thesis/dissertation

eScholarship.org Powered by the California Digital Library
University of California

Dynamic behaviors of progenitors and neurons in the gyrencephalic cortex

by

Caitlyn Cody Gertz

DISSERTATION

Submitted in partial satisfaction of the requirements for the degree of

DOCTOR OF PHILOSOPHY

in

Neuroscience

in the

[redacted]

Copyright (2015)

by

Caitlyn Cody Gertz

For my parents and grandmother, Dorothy

Acknowledgements

First, I would like to thank my mentor and thesis advisor, Arnold Kriegstein, without whom this work would not have been possible. Arnold graciously took me in when I needed to change thesis labs during my second year, and he has continued to be supportive throughout my graduate studies. He has allowed me to work independently and develop my own interests, but was always available when I needed guidance. This flexible mentoring approach helped me to mature scientifically and personally. I am especially grateful for Arnold's support of my professional endeavors outside of the lab.

I would also like to thank my thesis committee members: John Rubenstein, Sam Pleasure, and Arturo Alvarez-Buylla. John kindly served as my committee chair and was a consistent source of encouragement throughout my graduate career. In addition to providing valuable insights during committee meetings, my Genentech internship would not have been possible without Sam's support. I appreciate Arturo's meaningful feedback that encouraged me to consider the broader impact of my work. I would also like to thank David Hansen for serving as my additional committee member and for being a valuable resource during my early years in the Kriegstein lab.

I am indebted to Kriegstein lab members and colleagues in Pod D who provided an intellectually stimulating and endlessly entertaining work environment. All of the postdocs I have overlapped with have provided invaluable scientific feedback and made the lab a fun and exciting place to work. I would particularly like to thank Corey Harwell and Lakshmi Subramanian for helping me find my way when I first joined the lab. William Walantus and Yingying Wang provided crucial technical support that enabled my projects to move forward. My fellow graduate students in the lab, Jan Lui

and Bridget Ostrem, were instrumental in making my time in Arnold's lab truly enjoyable.

I would also like to thank the UCSF Neuroscience community, which is a vital research environment that I am privileged to have been a part of. Previously directed by Louis Reichhardt and now under the leadership of Roger Nicoll, the Neuroscience Graduate Program provided fundamental support throughout my studies. Along with the leadership, I am grateful for the wonderful administrative support provided by Pat Veitch, Carrie Huckaba, and Lucita Nacionales, which was critical to the program's success. I was drawn to UCSF by the diverse group of talented graduate students, many of whom I've formed close friendships with. I am particularly grateful for the support and companionship of my classmates and would specifically like to thank Kate Lovero, without whom I wouldn't have made it through this journey.

Several mentors inspired my scientific interests throughout my academic career. I would like to thank Richard Seegal and Anne Dreiem for providing my first experience in a neuroscience lab and for having confidence in my research abilities. I would also like to thank Susan Wray for challenging me to think creatively and independently. Under the guidance of Joseph Corey, I learned how to synthesize a project, design experiments, and prepare a manuscript. Without Joe, as well as the additional support of Eva Feldman, I would not have had the opportunity to pursue my PhD at UCSF.

Several people, both in San Francisco and across the country, have made this accomplishment possible. Specifically, I would like to thank Jeff Hendricks and his family for encouraging my scientific endeavors and supporting me in the beginning of my PhD. I am grateful for Greg Romero's confidence in my ability to complete my PhD and his understanding of the demands of graduate school. Ruby Hsu was my mentor during a first year rotation and we have been close friends ever since. I am grateful for her companionship and wouldn't have enjoyed this journey nearly as much without her by my side. Dan has been my confidant and biggest supporter since high school. Although residing nearly 3000 miles away, he is always there to listen and knows exactly what to say when the going gets tough. He makes me want to be a better person and live life to the fullest.

Lastly, none of this could have been possible without the unwavering support of my family. I have always looked up to my brother Jason Gertz, a fantastic scientist and an even better person. Him and his talented wife K-T Varley have supported all of my professional and personal endeavors and provided invaluable insights throughout my graduate career. Words cannot adequately express my gratitude to my parents Sue and Ken Gertz. They have provided endless support and have always believed in my ability to conquer what I set out to achieve. I wouldn't be where I am today without their unconditional love and guidance and I am forever grateful.

Contributions

All of the work described in this dissertation was done under the direct supervision and guidance of Arnold Kriegstein. The time-lapse imaging experiments in Figure 5 of Chapter 3 were carried out by Jan Lui and Bridget Ostrem. All other experiments were carried out by Caitlyn Gertz. I designed the schematic in Figure 8 of Chapter 3, which was executed by Kenneth Probst using Adobe Illustrator. Technical assistance was provided by William Walantus and Yingying Wang.

The work in Chapter 3 has previously been published in *The Journal of Neuroscience* and is reproduced with permission:

Gertz CC, Lui JH, LaMonica BE, Wang X, Kriegstein AR. 2014. Diverse behaviors of outer radial glia in developing ferret and human cortex. *The Journal of neuroscience* **34**(7): 2559-2570.

ABSTRACT OF THE DISSERTATION

Dynamic behaviors of progenitors and neurons in the gyrencephalic cortex

By Caitlyn Cody Gertz

Doctor of Philosophy in Neuroscience

University of California, San Francisco, 2015

The evolutionary expansion of the mammalian cerebral cortex is responsible for our unique higher cognitive abilities such as language and conscious thought. Developmental changes in neural progenitor composition likely contributed to the increased size and number of neurons in the primate cortex. For instance, a germinal region, referred to as the subventricular zone (SVZ), is greatly expanded in primates and contains a heterogeneous population of neural progenitors, including outer radial glia (oRGs). Since oRGs are more abundant in the primate than the rodent and contribute to neurogenesis, an increase in this cell population is thought to underlie cortical expansion and folding. However, the specific contribution of oRGs and other cell populations, such as neurons, to the size and shape of the adult mammalian cortex remains unknown. Since the ferret is gyrencephalic, possesses an enlarged SVZ with an abundance of oRGs, and is experimentally tractable, it provides an attractive model for studying cortical expansion and folding. Here, I provide a detailed characterization of progenitor and migrating neuron behaviors in the developing ferret cortex. I present data demonstrating the mitotic behaviors, proliferative capacity, and daughter cell fates of ferret oRGs and highlight morphological diversity within this progenitor population. I go on to present a technique for visualizing neurogenic divisions and neuronal migration in the ferret cortex. I describe neuronal migration properties that appear to differ from the rodent, such as greater variation in the direction of migration and increased meandering, specifically at later ages when the ferret cortex has begun to fold. These data provide a framework for future studies using the ferret to elucidate the cellular and molecular mechanisms of cortical expansion and folding, as well as neurodevelopmental diseases.

Table of Contents

Acknowledgements……………..…………………………………………………………iv

Contributions…………………….………………………………………….…………….…vii

Abstract …………...……….……………………………………………………………...viii

List of Figures...……………….....……………………………………………...……......xiv

CHAPTER 1 – General Introduction 1

Cerebral cortical development and theories of evolutionary expansion…...…......2

Role of the SVZ in cortical expansion and folding……..……………..……………….5

Ferret as a model system for studying cortical expansion and folding……..……..9

CHAPTER 2 – Methods 14

Preparation of cortical slice cultures……………………………………….…………...15

Viral infection and time-lapse imaging of cortical slice culture.……………...…...15

Ex utero electroporation.……………………………………………..………......16

Immunohistochemistry and confocal imaging……………………………………….….16

Cell counts…………………...……………………………………………………….…17

Analysis of cell divisions in cortical slice cultures labeled with AV-CMV-GFP...17

Analysis of neuronal migration in cortical slice cultures labeled with AAV2-CAG-GFP……………………………………………………………………………18

Graphs and statistics………………………………………………………………..19

CHAPTER 3 – Diverse behaviors of outer radial glia in developing ferret and human cortex 21

Summary…………………………………………………………………….……………22
Introduction………………………………………………………..……………..23
Results………………………………………………………………………..…25
SVZ divisions in the developing ferret cortex………………………..............25
MST divisions are found throughout the VZ and SVZ……………….............27
Ferret oRG division angle relative to the VZ varies, whereas division angle relative to the primary fiber remains constant………………..………..............28
Ferret oRG fibers are dynamic and do not always contact the pial surface....29
Human oRGs exhibit diverse behaviors similar to the ferret………...............31
Daughters of ferret oRGs undergo multiple rounds of divisions and remain undifferentiated………………..………..32
Discussion………………………………………………………………………..…36

CHAPTER 4 – Neuronal migration dynamics in the developing ferret cortex 61

Summary……………………………………………………………………………..62
Introduction………………………………………………………………………….63
Results……………………………………………………………………………..66
AAV2-CAG-GFP labels migrating neurons in the developing ferret cortex...66
Populations of slow and fast neurons migrate within the developing ferret

cortex……………………………………………………………………………......67

Cortical plate-directed radial migration of ferret neurons decreases with age……………………………………………………………………………...68

Neuronal migration routes become more tortuous at later ages……………...70

Ferret neurons can migrate promiscuously along different radial glia fibers...70

Divisions by AAV2-CAG-GFP labeled progenitors are neurogenic.................71

Discussion……………………………..……………………...............………..…..73

CHAPTER 5 – General Conclusion 91

REFERENCES 96

List of Tables

CHAPTER 3

Table 1 – Comparison of post-time-lapse oRG daughter cell fates between ferret and human……………………………………………………………………………..57

List of Figures

CHAPTER 3

Figure 1 – SVZ divisions in the developing ferret cortex……………………..………..…..41

Figure 2 – MST divisions can be found throughout the VZ and SVZ..………….……….43

Figure 3 – oRG division angles vary with respect to the VZ surface but remain constant with respect to the primary fiber.........…...….……………………………….…….45

Figure 4 – oRG fibers are dynamic during the cell cycle and do not always contact the pial surface……………………..…..….…..…..….…...….…..….……..….…….47

Figure 5 – Human oRGs exhibit diverse behaviors similar to the ferret………………..…49

Figure 6 – oRG daughters can undergo multiple rounds of divisions………………..…...51

Figure 7 – The majority of oRG daughters remain undifferentiated....…..…..…..……..……53

Figure 8 – Model of diverse oRG behaviors and daughter cell fates during cortical development…………………………………………………………………..55

Movie 1 – Ferret oRGs undergo MST and stationary divisions…..…...………….…..…….59

Movie 2 - RG cells within the ferret VZ divide both at the VZ surface and subapically...59

Movie 3 – Ferret oRGs undergo multiple rounds of self-renewing divisions……………60

CHAPTER 4

Figure 1 – AAV2-CAG-GFP labels migrating neurons in the developing ferret cortex..79

Figure 2 – Populations of fast and slow migrating cells can be detected in the ferret cortex..81

Figure 3 – Cortical plate-directed radial migration of ferret neurons decreases with age...83

Figure 4 – Straightness of neuronal migration decreases with age..........…..………....…85

Figure 5 – Ferret neurons can migrate promiscuously along different radial glial fibers………………………………………………………………………...87

Figure 6 – AAV2-CAG-GFP-positive cell divisions are IPC-like …………...………....…89

CHAPTER 1:

General Introduction

Cerebral cortical development and theories of evolutionary expansion

The brain is the most complex organ of vertebrates responsible for the centralized control of behavior through the integration of sensory input from an organism's environment. The cerebral cortex, which lines the surface of the forebrain, contains numerous cell bodies, including neurons. In mammals, it is the most highly evolved brain region and sometimes exhibits a folded morphology, termed gyrencephaly, which gives a larger cortical surface area in the confined volume of the skull. The massive expansion of the cerebral cortex and the huge increase in number of neurons enables our unique higher cognitive abilities such as planning and decision-making (Hofman, 2014).

The mammalian cerebral cortex has an intricate cytoarchitecture consisting of six horizontal layers, each containing distinct neuronal types and synaptic connections. The generation of this adult structure requires the coordination of complex developmental events. Pyramidal neurons, the main excitatory neurons of the mammalian cortex, are born in subcortical germinal regions adjacent to the ventricular surface. Immature neurons must migrate, sometimes over long distances, to reach the appropriate layer within the cortex (Angevine and Sidman, 1961; Luskin and Shatz, 1985; Rakic, 1974). Following the formation of the cortical plate (CP), the cortex develops in an "inside-out" manner, in which upper layer neurons are born after deeper layer neurons and must migrate past them to reach their final destination (Ayala et al., 2007; Marin and Rubenstein, 2003; Marin et al., 2010).

Early observations revealed the close apposition of migrating pyramidal neurons with fibers of radial glia (RGs) whose cell bodies are located adjacent to the ventricle in a germinal region referred to as the ventricular zone (VZ). From these findings it was proposed that the fibers of RGs, which span to the pial surface, serve as guides for neuronal migration (Edmondson and Hatten, 1987; Rakic, 1971, 1972; Rakic et al., 1974). This theory was corroborated by studies in the rodent, where time-lapse imaging revealed the radial glia-guided migration of pyramidal neurons to the CP (Noctor et al., 2001).

It was originally believed that a cell population residing within the VZ, but separate from RGs, function as neuronal precursors (Bentivoglio and Mazzarello, 1999; Levitt et al., 1981). Evidence from songbirds first demonstrated the role of RGs in neurogenesis (Alvarez-Buylla et al., 1988, 1990). However, this concept was not fully accepted until a little over a decade ago, when it was established that RGs not only provide physical guides for migration, but are also the neural progenitors giving rise to pyramidal neurons (Malatesta et al., 2000; Miyata et al., 2001; Noctor et al., 2001). Studies in the rodent revealed that RGs generate neurons by self-renewing asymmetric divisions, and that immature neurons migrate along RG fibers, often those belonging to the parent cell, to reach the CP (Noctor et al., 2001; Noctor et al., 2004; Noctor et al., 2008). These observations helped refine the original 'radial unit hypothesis' regarding the cellular mechanisms responsible for the evolutionary expansion of the mammalian cerebral cortex (Rakic, 1988, 1995).

According to this model, an initial increase in symmetric, self-renewing divisions first by neuroepithelial cells and then by RGs serves to increase the number of founder cells within the VZ. At later stages during neurogenesis, an increase in the number of asymmetric divisions increases neuronal numbers. Moreover, this model proposes that neurons migrate along nearby RG fibers resulting in the formation of ontogenetic columns and the creation of a 'protomap' from the VZ founder cells onto the developing cortex (Rakic, 1995, 2009). Experimental findings in the rodent supported this theory, providing evidence that by increasing RG abundance (Chenn and Walsh, 2002, 2003) or reducing RG cell death (Haydar et al., 1999; Kuida et al., 1996; Roth et al., 2000) one could increase the number of radial units and produce a larger cortical surface area with folds (Rakic, 2003). However, this model predicts a proportional increase in ventricular surface area during neurogenic stages to accompany the increase in cortical surface area. This was shown experimentally in the embryonic rodent expressing constitutively active Notch (Chenn and Walsh, 2002), but is not a naturally occurring morphology of the gyrencephalic brain (Kriegstein et al., 2006). Therefore, it is unlikely that this mechanism alone accounts for the massive cortical expansion observed in primates.

The discovery of an additional neural progenitor subtype suggested that the 'radial unit hypothesis' was overly simplified. In addition to giving rise to neurons directly, RGs in the rodent were found to generate intermediate progenitor cells (IPCs) (Haubensak et al., 2004; Noctor et al., 2004). IPCs divide within the VZ or the subventricular zone (SVZ), a second germinal region located just basal to the VZ. In the rodent, IPCS undergo a single, symmetric division to produce a pair of neurons (Noctor et al., 2004). After the identification of IPCs, an alternative model regarding the evolutionary expansion of the mammalian cortex was proposed, termed the 'intermediate progenitor hypothesis' (Kriegstein et al., 2006).

According to this model, an increase in asymmetric divisions by RGs increases the number of neurons in the radial dimension, while an increase in IPC divisions tangentially increases cortical surface area (Kriegstein et al., 2006). Since this hypothesis does not require an increase in the number of RGs within the VZ, it is consistent with the morphology of the adult gyrencephalic cortex, which lacks a proportional increase in ventricular surface area. Additionally, observations in the primate have revealed a greatly expanded SVZ region during development (Lukaszewicz et al., 2005; Smart et al., 2002), which is thicker in areas underlying future gyrus formation (Kriegstein et al., 2006). Together these findings support the role of SVZ expansion in neocortical enlargement.

Role of the SVZ in cortical expansion and folding

While studies have documented the increased size of the primate SVZ, the characterization of cells within this region remains an active area of research. The primate SVZ can be divided into an inner (ISVZ) and outer (OSVZ) region separated by a thin fiber layer. The OSVZ displays cellular heterogeneity and contains both progenitor cells and immature, migrating neurons. Markers used to identify RGs and IPCs in the rodent revealed the presence of both of these cell types within the primate OSVZ (Bayatti et al., 2008; Mo and Zecevic, 2008; Zecevic et al., 2005). RG-like cells within the OSVZ were termed outer radial glia (oRG), due to their basal, SVZ location. Similar to RGs residing within the VZ (vRGs), oRGs possess a basal fiber that extends towards the pial surface. However, unlike vRGs, they lack an apical process contacting the ventricle (Fietz et al., 2010; Hansen et al., 2010). Time-lapse imaging in human fetal cortical slices revealed that oRGs exhibit a unique mode of division termed mitotic somal translocation (MST) (Hansen et al., 2010), which is distinct from interkinetic nuclear migration of vRGs (LaMonica et al., 2013; Miyata et al., 2001; Noctor et al., 2001) and stationary divisions of IPCs (Hansen et al., 2010; Noctor et al., 2004). During MST, the cell body moves rapidly along the basal fiber prior to cytokinesis (Hansen et al., 2010). This mode of division may be essential for expansion of the SVZ during development (Ostrem et al., 2014). Human oRGs were found to undergo symmetric, self-renewing divisions that expanded the progenitor population, as well as asymmetric divisions that produced IPC daughters (Hansen et al., 2010). In addition, dynamic imaging revealed the generation of oRGs by vRGs undergoing horizontal divisions, revealing an additional source of oRG production (LaMonica et al., 2013).

The discovery of an enlarged primate SVZ composed of oRGs and IPCs lead to an updated hypothesis regarding the cellular mechanisms responsible for the evolutionary expansion of the mammalian cerebral cortex. In addition to an increase in IPC divisions, as proposed by the 'intermediate progenitor hypothesis' (Kriegstein et al., 2006), a further amplification in neuronal production could be achieved by an increase in both the generation of oRGs and asymmetric oRG divisions that produce IPCs (Fish et al., 2008; Lui et al., 2011). This model is supported by studies revealing a positive correlation between SVZ proliferation and neocortical size and gyrification (Lewitus et al., 2013; Reillo et al., 2011). Additionally, an enlarged SVZ with a substantial population of oRGs was discovered in non-primate gyrencephalic species, such as the ferret (Fietz et al., 2010; Reillo and Borrell, 2012; Reillo et al., 2011). This further supports the hypothesis that an increase in SVZ size, accompanied by an increase in oRGs, may be a common evolutionary mechanism by which an enlarged, folded cortex developed.

Although this hypothesis incorporates our most current understanding of mammalian cortical development, it may be overly simplified. For instance, while oRGs appear necessary for cortical expansion and folding, they are not sufficient. The lissencephalic, or smooth brain, rodent possesses a modest population of oRG cells during neurogenesis (Martinez-Cerdeno et al., 2012; Shitamukai et al., 2011; Wang et al., 2011). In addition, the marmoset, a lissencephalic primate, has abundant oRGs during cortical development (Garcia-Moreno et al., 2012; Kelava et al., 2012). Further evidence suggesting that oRG abundance does not predict adult cortical morphology, comes from studies demonstrating species-specific oRG behaviors. While oRGs in the human self-renew and produce IPCs (Hansen et al., 2010), oRGs in the mouse appear to self-renew and produce neurons directly (Wang et al., 2011). Moreover, the proliferative capacity of oRGs may differ between species, causing variations in daughter cell production. In addition to cell cycle dynamics, the primary function of oRGs may be species-dependent. Human oRGs have been proposed to contribute to both neurogenesis and neuronal migration (Lui et al., 2011), while static imaging studies suggest that ferret oRGs strictly serve as scaffolds for neuronal migration (Borrell and Reillo, 2012). Together these findings suggest that oRG abundance does not predict the size and shape of the adult mammalian cortex. Rather, a combination of factors, including proliferative potential, daughter cell fates, and primary function, likely determine the contribution of oRGs to cortical development.

Although remarkable progress has been made in our understanding of mammalian cortical development, the contribution of specific progenitor subtypes to cortical expansion and folding remains unknown. Although snapshots of the lineage progression from vRG to SVZ progenitor (oRG or IPC) to mature neuron have been observed in the primate (Betizeau et al., 2013; Hansen et al., 2010; LaMonica et al., 2013), experimental limitations have precluded the documentation of the entire process in real-time. Therefore, the relative contribution of SVZ progenitor subtypes to neuronal output has yet to be determined. It has been proposed that IPCs and oRGs have different roles in shaping adult cortical topography and that distinct SVZ progenitors are responsible for the development of discrete cortical properties including thickness, surface area, and folding (Nonaka-Kinoshita et al., 2013). This hypothesis assumes that these properties are independent variables; however, neocortical surface area and gyrification are positively correlated and intimately connected (Lewitus et al., 2013; Zilles et al., 2013). Moreover, since oRGs can produce IPCs these progenitor subtypes lie within the same lineage, making it difficult to dissociate their individual contributions to cortical development.

In addition to SVZ progenitors, the relative contribution of vRGs to the development of a folded cortex remains unknown. As the SVZ becomes much larger than the VZ during development of the gyrencephalic cortex, it has been assumed that SVZ progenitors, including oRGs and IPCs, become the major source of neurons during upper layer neurogenesis (Florio and Huttner, 2014; Lui et al., 2011). However, vRGs may continue to produce a substantial number of neurons either directly or indirectly during this stage. This raises important questions regarding the dynamics of pyramidal neuron migration in the gyrencephalic cortex. For example, how do neurons born at the same time but by progenitors residing in different germinal zones, such as the VZ versus OSVZ, end up in the same cortical layer? These cells would have very different migratory routes and distances to travel. It is unclear how this process is coordinated in species with a folded cortex.

According to the prevailing model of neuronal migration, newborn pyramidal neurons assume a bipolar morphology and migrate radially along vRG fibers to reach the cortex (Evsyukova et al., 2013). Specifically, it has been proposed that neurons may migrate along the fiber of their parent cell, thereby maintaining a spatial relationship between clonally related neurons (Noctor et al., 2001; Rakic, 1988). However, retroviral studies in the ferret (Reid et al., 1997; Ware et al., 1999) and primate (Kornack and Rakic, 1995) have demonstrated the tangential dispersion of clonally related neurons, suggesting that they do not always adhere to strict radial pathways during migration. Furthermore, it is possible that neuronal migration properties differ in a smooth versus folded brain due to variations in cortical topography; however, this remains unknown. For instance, an expanded SVZ in gyrencephalic species increases the distance neurons must migrate to reach the cortex. Additionally, an abundance of oRGs, whose fibers presumably support neuronal migration, expands and complicates the radial fiber scaffold. Moreover, gyri and sulci begin forming while neurons are still being produced, further complicating the migratory landscape. These features may result in neuronal migration dynamics that differ from the current model deduced primarily from rodent studies. Several neurodevelopmental disorders are caused by defective neuronal migration. In one such disorder, termed lissencephaly, patients do not develop proper gyri and sulci. This suggests that in addition to progenitor dynamics, the regulation of neuronal migration is crucial for the development of gyrencephaly (Ross and Walsh, 2001).

Ferret as a model system for studying cortical expansion and folding

An appropriate animal model is necessary to further our understanding of the cellular and molecular mechanisms responsible for the evolutionary expansion and folding of the mammalian neocortex. While much has been learned about cortical evolution from the use of primate samples, studies have primarily been limited to the use of fixed tissue and static analyses. Time-lapse imaging has recently been adopted to monitor cell behavior in the intact cortex of the human (Hansen et al., 2010; LaMonica et al., 2013; Ostrem et al., 2014) and primate (Betizeau et al., 2013), but these studies are restricted in length due to tissue viability. Moreover, even though the ability to culture primate cortical tissue enables gene knockdown or overexpression studies, they can only be performed transiently. Therefore, the long-term effects of genetic perturbations cannot be determined. A suitable animal model for studying cortical expansion and folding must possess a large, folded cortex and be experimentally tractable.

The ferret (*Mustela putorius furo*) is a gyrencephalic carnivore that is closely related to the weasel. Since they share many anatomical features with humans, they have frequently been used in biomedical research (Moody et al., 1985). For instance, the ferret cerebral cortex displays a characteristic pattern of cortical folds. The formation of gyri and sulci begins postnatally (Smart and McSherry, 1986a, b) and neocortical neurogenesis continues until postnatal day 14 (Jackson et al., 1989; McConnell, 1988). During neurogenesis, ferrets develop an expanded cortical SVZ, which according to static marker expression analyses possesses an abundance of oRGs and IPCs (Fietz et al., 2010; Reillo and Borrell, 2012; Reillo et al., 2011). Although rodents are more closely related to primates than carnivores, the folded morphology of the adult ferret cortex, along with the presence of an enlarged SVZ is more reminiscent of the primate. As such, the ferret could serve as a model for studying the cellular mechanisms leading to cortical expansion and folding.

In addition, the ferret can be manipulated experimentally at both embryonic and postnatal ages. Ferret gestation is approximately 42 days, with females having average litter sizes of 3 to 7. Viruses can be delivered into the ventricular space and germinal regions of both embryonic and postnatal animals (Nonaka-Kinoshita et al., 2013; Reid et al., 1997; Reillo et al., 2011; Ware et al., 1999). This allows the analysis of lineage relationships and the behaviors of clonally related cells. Plasmid DNA can also be delivered and targeted to different cell populations by electroporation (Borrell, 2010; Kawasaki et al., 2013; Nonaka-Kinoshita et al., 2013; Reillo et al., 2011). This allows the introduction of shRNAs and overexpression constructs at various stages of development. Due to the recent publication of the draft genome sequence of the ferret (Peng et al., 2014), these experiments can be more easily performed. The effects of gene knockdown can be monitored over time, until the animal reaches maturity and adult cortical morphology is acquired. In addition, techniques are being developed to genetically engineer ferrets (Sun et al., 2014), which will enable a more precise control of gene overexpression and/or knockdown. The experimental accessibility of the ferret enables the exploration of molecular mechanisms responsible for the evolutionary expansion and folding of the mammalian neocortex. It also enables the study of disease genes that are linked to human neurodevelopmental disorders.

Several diseases are associated with the improper development of the cerebral cortex. For example, defective neuronal migration is the cause of a group of conditions collectively referred to as neuronal migration disorders. Lissencephaly is one such disorder, in which children do not develop proper gyri and sulci and generally experience developmental delays and seizures. In microcephaly, patients have a significantly reduced brain size but display proper cortical folding, and typically present with neurological defects and seizures. Both of these neurodevelopmental disorders have genetic causes that have been modeled in the rodent (Ross and Walsh, 2001). While these studies have provided insight into mechanisms leading to disease development, genetic mutations that cause these severe phenotypes in the human typically cause little to no phenotypes in the rodent. Since the rodent brain is inherently lissencephalic and lacks an expanded SVZ with abundant neural progenitors, it may not be an adequate model for studying human cortical development. Although ferrets diverged from humans earlier than mice, the ferret may provide a more suitable model for elucidating the cellular and molecular mechanisms that cause human neurodevelopmental diseases.

The first step in implementing the ferret as a model system of cortical expansion and folding is to examine the behaviors of progenitors in the developing ferret cortex. While static marker expression analyses have been performed, the behaviors of ferret progenitors, including oRGs, have not been assessed in real-time. Previous studies suggest that progenitor abundance alone does not predict adult cortical topography and that progenitor behaviors are species-specific. Therefore, a comprehensive analysis of ferret progenitor behaviors is necessary for comparison to the primate. In addition, as lissencephaly results from defective neuronal migration, neuronal migration properties likely contribute to the development of gyrencephaly. However, a thorough analysis of neuronal migration dynamics in gyrencephalic species has not been performed. Due to the experimental accessibility of the ferret, it provides an attractive model for elucidating mechanisms of neuronal migration in a folded cortex.

The aim of my graduate work was to study ferret cortical development in order to establish the ferret as a model system for studying both the evolutionary expansion of the cerebral cortex, as well as human neurodevelopmental diseases. Specifically, I used time-lapse imaging to perform a comprehensive analysis of ferret progenitor behaviors. In chapter 3, I describe the dynamic morphologies, mitotic behaviors, and daughter cell fates of ferret oRGs during upper layer neurogenesis. I highlight diversity within the ferret and human oRG populations in terms of location, morphology including fiber orientation, and mitotic dynamics. In chapter 4, I present a novel technique for visualizing neurogenic divisions and neuronal migration in the ferret in real-time. Using this method, I describe pyramidal neuron migration and show that neurons exhibit a decrease in radial migration towards the CP, as well as an increase in meandering along the migratory route, at later ages when the ferret cortex begins to fold. I describe ferret pyramidal neurons migrating along, and switching between, several different RG fibers, providing a mechanism by which neurons may tangentially disperse in the developing gyrencephalic cortex. I hope that this work will enhance our understanding of gyrencephalic cortical development and aid in future studies using the ferret to model neurodevelopmental disorders.

CHAPTER 2:

Methods

Preparation of cortical slice cultures

As previously described (Hansen et al., 2010; LaMonica et al., 2013), human fetal brain tissue was collected at San Francisco General Hospital and transported to the laboratory for further processing. Collections were made with previous patient consent and following all legal and institutional ethical regulations approved by the UCSF Committee on Human Research (institutional review board). Embryonic day (E) 27 timed-pregnant ferrets were obtained from Marshall BioResources (North Rose, NY) and maintained according to protocols approved by the UCSF Institutional Animal Care and Use Committee. E39 pregnant dams were deeply anesthetized with ketamine followed by isoflurane administration. Ovariohysterectomy for fetus collection was then performed and embryonic brains, along with meninges, removed in chilled artificial CSF (ACSF; 125 mM NaCl, 2.5 mM KCl, 1 mM MgCl2, 2 mM CaCl2, 1.25 mM NaH2PO4, 25 mM NaHCO3, 25 mM d-(+)-glucose, bubbled with 95% O2/5% CO2). Postnatal day (P) 0 corresponded to the day of birth. P2 to P7 ferret kits were deeply anesthetized with isoflurane, decapitated, and the brain extracted and meninges removed in chilled artificial ACSF. Ferret and human brain tissue was embedded in 3.5% low melting point agarose in ACSF and 250–300 µm coronal vibratome sections transferred to Millicell-CM slice culture inserts (Millipore) that were immersed in cortical slice culture medium (66% BME, 25% Hanks, 5% FBS, 1% N-2, 1% penicillin, streptomycin and glutamine, all Invitrogen, and 0.66% D-(+)-glucose, Sigma-Aldrich).

Viral infection and time-lapse imaging of cortical slice cultures

Adenoviruses (AV-CMV-GFP, AV-CMV-mcherry, 1 x 10^{10}) at a dilution of 1:50–1:500 and an adeno-associated virus (AAV2-CAG-GFP, 1 x 10^{13}) at a dilution of 1:10-1:50 (Vector Biolabs) were applied to cortical slices that were then cultured at 37°C, 5% CO2, 8% O2. For quantification of AV-CMV-GFP-labeled oRGs and AAV2-CAG-GFP-labeled cells, ferret slices were then fixed in 4% PFA in PBS overnight and processed for immunohistochemistry. For time-lapse imaging, cultures were then transferred to an inverted Leica TCS SP5 confocal microscope with an on-stage incubator streaming 5% CO2, 5% O2, balance N2 into the chamber. Slices were imaged using a 10x or 40x air objective at 15–45 min intervals for up to 5 days with repositioning of the z-stacks every ~12 h.

Ex utero electroporation

P7 ferret kits were deeply anesthetized with isoflurane, decapitated, and the brain extracted and meninges removed in chilled artificial ACSF. A micropipette was used to inject 1-2 μl of CMV-tdtomato plasmid DNA (1.5μg) into the ventricle of both hemispheres. The positive paddle of the electrode was placed on the lateral cortex and 5 pulses at 52mV applied (50ms with 1 sec intervals). Brains were immediately transferred to fresh, chilled ACSF and processed for cortical slice cultures.

Immunohistochemistry and confocal imaging

Cortical slice cultures were fixed in 4% PFA in PBS overnight and then stored in PBS plus 0.01% sodium azide at 4°C. Slices were subjected to boiling citrate-based antigen retrieval solution (Vector Laboratories) for 20 min and permeabilized and blocked in blocking buffer (PBS plus 0.1-2% Triton X-100, 10% serum, and 0.2% gelatin) for 1 h. Primary antibodies were diluted in blocking buffer and applied to slices for 36-72 h at 4°C. Slices were washed with PBS plus 0.5% Triton X-100 and then incubated in secondary antibodies diluted in blocking buffer for 4-36 h. Images were acquired on a Leica TCS SP5 X laser confocal microscope. Primary and secondary antibodies used: mouse anti-Satb2 (Santa Cruz Biotechnology, sc-81376, 1:250), goat anti-SOX2 (Santa Cruz Biotechnology, sc-17320, 1:250), rabbit anti-TBR2 (Abcam, ab23345, 1:100), chicken anti-GFP (Aves Labs, GFP-1020, 1:1000), rabbit anti-OLIG2 (Millipore AB9610, 1:250), mouse anti-OLIG2 (Millipore, MABN50, 1:100), rabbit anti-Lhx6 (Vogt et al., 2014), mouse anti-KI67 (Dako F0788, 1:200), AlexaFluor 488, 546, 594, or 647- conjugated donkey anti-goat, -rabbit, -mouse IgG (Invitrogen, 1:500), and AlexaFluor 488 donkey anti-chicken IgY (Jackson ImmunoResearch, 1:500).

Cell counts

Imaris software was used to count and determine the percentage of AV-CMV-GFP and AAV2-CAG-GFP-positive cells expressing different markers. For each virus, at least 3 (and up to 5) slices were counted per marker in a region spanning the ventricular zone (VZ) to the end of the cortical plate (CP). The percentage of GFP-positive cells was calculated per slice and averaged between slices, with a total of 432 - 1182 cells analyzed per marker.

Analysis of cell divisions in cortical slice cultures labeled with AV-CMV-GFP

Maximum intensity projections of the collected stacks (5-10μm step size) were compiled, generated into movies, and analyzed using Imaris software. Four imaged positions of frontal-parietal lateral cortex from two P3 non-littermate of either sex, and four imaged positions of the same region from one E39 ferret of either sex were examined. For each P3 position the VZ surface was visible and all divisions that occurred between the start of imaging and 48 h later were analyzed (number of cells analyzed (n)=512). The distance of the cell from the VZ surface before the division was measured. MST length was measured as the distance between the site of cytokinesis and the center of the soma before the onset of translocation. Using Screen Protractor (Iconico), division angles were determined by calculating the angle between cytokinesis and the ventricular surface ("division angle relative to the VZ"). For MST divisions, the angle between cytokinesis and the primary fiber (the fiber along which the cell body translocated) was also calculated ("division angle relative to the primary fiber") (n=174). An additional position was used for analysis of divisions at the VZ surface at P3 (n=12). Five imaged positions from three different human samples, gestational week (GW) 17.5-18, that contained the OSVZ were used to determine the angle between cytokinesis and the adjacent radial fiber scaffold for MST divisions ("division angle relative to the radial fiber scaffold") (n=71). Three imaged positions from two human samples, GW 16-16.5, were used for analysis of divisions at the VZ surface (n=57).

Analysis of neuronal migration in cortical slice cultures labeled with AAV2-CAG-GFP

Eight AAV2-CAG-GFP labeled imaging fields of frontal-parietal lateral cortex from four P2/3 non-littermate ferrets of either sex, and 12 imaged positions of the same region from three P6/7 non-littermate ferrets of either sex were analyzed. The location of the imaged fields spanned the entire cortex from the VZ to the CP. Maximum intensity projections of the collected stacks (5–10 μm step size) were compiled, generated into movies, and analyzed using Imaris software. ImarisTrack was used to automatically generate tracks of GFP-positive cells over time. Tracks were then manually edited to correct for software error and the z positions set to a constant value so that only the x and y values of a track changed over time. Track statistics, including track duration, length, average speed, straightness, and displacement, were generated by the software and exported for further analysis. The direction of migration was determined using the x, y displacement values of the last time-point of a track. According to these values, each track was assigned to a quadrant, with positive x and y values assigned to quadrant I, negative x and positive y to quadrant II, negative x and y to quadrant III, and positive x and negative y to quadrant IV. The x, y coordinates were then converted into polar coordinates using the equation $\tan^{-1}(y/x)$, and the angle adjusted according to quadrant (no adjustment for tracks in quadrant I, 180° added to tracks in quadrant II and III, and 360° added to tracks in quadrant IV). The direction of the cortical plate was set to 45°-135°, with angles adjusted for imaging fields in which the direction of the cortical plate differed from this orientation (Chapter 4, Figure 3).

Graphs and statistics

Box plot and column graphs (mean + SEM) were generated in Prism GraphPad, JMP, or Excel. Displacement graphs were made in Imaris. Rose plots were generated in Oriana with vector sum (r) indicated with a red arrow. A linear regression analysis followed by a t-test was used to determine the significance of the relationship between MST length and distance from the VZ. Using GraphPad, the ROUT method was used to determine outliers with a fast average migration speed (Q = 1%) (Motulsky and Brown, 2006). An unpaired t-test with Welch's correction was used to assess track straightness. A Watson Williams F test and Mardia-Watson-Wheeler test were used to assess the mean and distribution of the direction of migration, respectively.

CHAPTER 3:

Diverse behaviors of outer radial glia in developing ferret and human cortex

Summary

The dramatic increase in neocortical size and folding during mammalian brain evolution has been attributed to the elaboration of the subventricular zone (SVZ) and the associated increase in neural progenitors. However, recent studies have shown that SVZ size and the abundance of resident progenitors do not directly predict cortical topography, suggesting that complex behaviors of the progenitors themselves may contribute to the overall size and shape of the adult cortex. Using time-lapse imaging, we examined the dynamic behaviors of SVZ progenitors in the ferret, a gyrencephalic carnivore, focusing our analysis on outer radial glia cells (oRGs). We identified a substantial population of oRGs by marker expression and their unique mode of division, termed mitotic somal translocation (MST). Ferret oRGs exhibited diverse behaviors in terms of division location, cleavage angle, and MST distance, as well as fiber orientation and dynamics. We then examined the human fetal cortex and found that a subset of human oRGs displayed similar characteristics, suggesting that diversity in oRG behavior may be a general feature. Similar to the human, ferret oRGs underwent multiple rounds of self-renewing divisions but were more likely to undergo symmetric divisions that expanded the oRG population, as opposed to producing intermediate progenitor cells (IPCs). Differences in oRG behaviors, including proliferative potential and daughter cell fates, may contribute to variations in cortical structure between mammalian species.

Introduction

Evolutionary expansion of the mammalian neocortex has led to increased cortical surface area accompanied by varying degrees of folding (Zilles et al., 2013), and has been attributed to differences in the size and composition of embryonic germinal zones (Kriegstein et al., 2006; Molnar, 2011). Specifically, the subventricular zone (SVZ) is greatly expanded in gyrencephalic primates and can be subdivided into an inner and outer region, the latter of which is negligible in lissencephalic rodents (Bayatti et al., 2008; Dehay and Kennedy, 2007; Lukaszewicz et al., 2005; Martinez-Cerdeno et al., 2012; Smart et al., 2002; Zecevic et al., 2005). The SVZ contains both intermediate progenitor cells (IPCs), which undergo symmetric divisions to produce neurons (Haubensak et al., 2004; Miyata et al., 2004; Noctor et al., 2004), and outer radial glia cells (oRGs) (Fietz et al., 2010; Hansen et al., 2010; Reillo et al., 2011).

Similar to ventricular radial glia (vRGs), oRGs express radial glia markers but lack an apical attachment to the ventricular surface (Fietz et al., 2010; Hansen et al., 2010; Reillo et al., 2011; Shitamukai et al., 2011; Wang et al., 2011) and exhibit a distinct mode of division termed mitotic somal translocation (MST). During MST, the cell body moves rapidly up the basal fiber towards the cortical plate (CP) before undergoing cytokinesis (Hansen et al., 2010; LaMonica et al., 2013; Wang et al., 2011). oRGs self-renew and produce neurons directly (Wang et al., 2011) or indirectly through the production of IPCs, which in the human undergo transit amplifying divisions to increase neuron production (Hansen et al., 2010). An enlarged SVZ, accompanied by an increase in both oRGs and IPCs, may account for neuronal amplification and the tangential dispersion of neurons that contributes to cortical expansion and gyrification (Lui et al., 2011).

The contribution of the SVZ to cortical structure appears to be conserved between primate and non-primate gyrencephalic species. For example, the ferret is a gyrencephalic carnivore with an expanded SVZ that contains progenitor populations similar to primates (Fietz et al., 2010; Martinez-Cerdeno et al., 2012; Reillo and Borrell, 2012). However, the relative abundance of oRGs does not predict degree of gyrification (Garcia-Moreno et al., 2012; Kelava et al., 2012), and daughter cell fates differ between species. Revealing the proliferative potential and daughter cell fates of ferret oRGs will allow comparison to other species and further our understanding of oRG contributions to cortical development.

Here we show that ferret oRGs undergo multiple rounds of symmetric divisions and only rarely produce IPCs at the ages examined. In addition, they exhibit diverse behaviors in terms of their division mode, location, and cleavage angle, as well as fiber orientation and dynamics. A subset of human oRGs displays similar behavioral diversity, suggesting that this variation is a general feature of oRG progenitors in different gyrencephalic species. We propose that together with proliferative capacity and daughter cell identities, this range in oRG behavior may contribute to the size and shape of the adult neocortex.

Results

SVZ divisions in the developing ferret cortex

At ferret P3-6, layer II-III neurons are being produced, cortical folds are beginning to appear, and the inner (ISVZ) and outer SVZ (OSVZ) are highly developed and populated by progenitors, including IPCs and oRGs (Fietz et al., 2010; Jackson et al., 1989; Reillo and Borrell, 2012; Reillo et al., 2011). In the human, ferret, and mouse, oRGs have been defined by expression of radial glial markers, location in the SVZ, and morphology, including the presence of a basal fiber that persists during mitosis and the absence of an apical attachment to the ventricular surface (Fietz et al., 2010; Hansen et al., 2010; Wang et al., 2011). Dynamically, oRGs exhibit a behavior known as MST, in which the cell soma moves rapidly towards the CP along the basal fiber beginning ~1 h before cytokinesis (Hansen et al., 2010; LaMonica et al., 2013; Wang et al., 2011). For the current study, we relaxed our definition of oRGs to investigate all cells that have a RG-specific gene expression profile and exhibit MST, but that may not necessarily fit our previously strict morphological definition of the cell type. To visualize progenitor behaviors in the developing ferret cortex, organotypic slice cultures of P3 brains were labeled with an adenovirus-expressing GFP (AV-GFP) and imaged 24 h later using time-lapse confocal microscopy.

Slice cultures were fixed and stained following virus application to determine the progenitor populations labeled by AV-GFP and to distinguish VZ from SVZ divisions. The VZ was visualized as an ~100 μm-thick, dense band of Sox2-positive cells with scattered Tbr2-positive cells immediately adjacent to the cerebral ventricle. A cell layer with sparser Sox2 staining and a dense Tbr2-positive band, located basal to the VZ, indicated the ISVZ, and measured 150μm in thickness (100-250μm from the VZ surface).

Just basal to the ISVZ, the cell layer containing sparse Sox2 and Tbr2 labeling corresponded to the OSVZ and measured 400µm in thickness and was ~250µm-650µm from the VZ surface (Figure 1A) (Hansen et al., 2010; Martinez-Cerdeno et al., 2012; Reillo and Borrell, 2012). Together, Sox2-expressing progenitors, Tbr2-expressing IPCs (Englund et al., 2005), and Olig2-expressing precursors constitute the vast majority of cycling cells in the P0-P6 ferret SVZ (Reillo and Borrell, 2012; Reillo et al., 2011). Of the AV-GFP-positive cells located in the SVZ and within the cell cycle (Ki67-positive), 55.2% (n=299) expressed the neural stem cell marker Sox2 and lacked expression of Tbr2 and Olig2, a marker expression profile that can be used to identify oRGs (Hansen et al., 2010). This suggests that over half of the AV-GFP-labeled cycling cells are oRG progenitors (Figure 1A).

Division mode, location, and orientation were then analyzed for all GFP-positive cell divisions that occurred during the first 48 h of time-lapse imaging. In this study, all cells that displayed MST lengths of 6µm or greater were referred to as oRGs. In total, 485 SVZ divisions were documented, with 162 (33.4%) exhibiting MST lengths >6µm, the approximate radius of the soma (Figure 1C). Although the average MST length was 17.6µm, MST lengths showed a skewed distribution toward smaller distances, with the majority of MST divisions < 15µm (59.9%) (Figure 1B). Interestingly, we observed oRG divisions similar to those described in the human and mouse, in which the cell possesses a basal fiber that does not retract during mitosis and is inherited by the basal daughter, but that did not exhibit MST (Figure 1D) (Hansen et al., 2010; Wang et al., 2011). We refer to these divisions as stationary oRG divisions. Because 55.2% of AV-GFP-labeled cells within the cell cycle are oRGs according to marker expression analysis, and only 33.4% of AV-GFP-labeled cells divided via MST, it is possible that up to 21.8% of the ferret oRG population undergoes stationary divisions (Movie 1).

MST divisions are found throughout the VZ and SVZ

Although MST divisions were found throughout the SVZ, the majority occurred within 100-300µm from the VZ surface, with fewer MST divisions observed at greater distances from the VZ (Figure 2A). Sixty-six percent and 85% of MST divisions occurred between 100-300µm and 100-400µm from the VZ surface, respectively. A scatter plot with a linear regression line is shown in Figure 2B illustrating MST length as a function of the distance of the dividing cell from the VZ surface. There is a modest but significant negative relationship between MST length and distance from the VZ (r^2=0.03, p=0.023), suggesting that larger MST lengths tend to occur closer to the VZ surface.

In addition to MST divisions in the SVZ, we also observed MST divisions within the VZ. Specifically, 6.9% (12/174) of all MST divisions occurred within 0-100µm from the VZ surface. An example of this is shown in Figure 2D, in which a RG cell located at the VZ surface undergoes basal MST before dividing with a horizontal division angle (0-30°). The basal daughter inherits the basal fiber, migrates away from the VZ surface, and expresses Sox2, suggestive of oRG identity. We also observed RG cells undergoing mitosis at the VZ surface and dividing with an oblique or horizontal division angle. Similar to ventricular RG (vRG) cell divisions that produce oRGs in the human and mouse (LaMonica et al., 2013; Wang et al., 2011), the basal daughter of these divisions inherited the basal fiber and expressed RG markers (Figure 2C).

Of 12 divisions where the RG cell was located at the VZ surface, five exhibited MST lengths >6µm, with an average length of 13.6µm. Moreover, all of these MST divisions were at a horizontal angle (0-30°) with respect to the VZ surface. Therefore, oRGs are generated not only from RG cells undergoing mitosis at the VZ surface (LaMonica et al., 2013; Wang et al., 2011), but likely also from RG cells residing within the VZ that undergo MST (Movie 2).

Ferret oRG division angle relative to the VZ varies, whereas division angle relative to the primary fiber remains constant

In the human and mouse cortex, oRGs have been described as possessing a basal fiber reaching to the pial surface, undergoing basally directed MST, and dividing with a horizontal division angle with respect to the VZ surface (Hansen et al., 2010; Wang et al., 2011). Although these features were commonly displayed by ferret oRGs (Figure 1C), progenitors were also observed undergoing MST that was not basally directed, as well as undergoing MST followed by a non-horizontal division angle. For instance, 3.7% of MST divisions were apically directed (Figure 3E). Although the majority of MST divisions in the ISVZ and OSVZ exhibited a horizontal division angle relative to the VZ surface (0-30°), up to 29% divided with an oblique angle (30-60°), and up to 24% with a vertical angle (60-90°) (Figure 3A, D). We observed oRGs with tangentially oriented fibers being generated from MST divisions within the SVZ. An example of this is shown in Figure 3C, in which an oRG cell with a basal fiber undergoes MST with a horizontal division angle to produce daughter cells that extend fibers parallel to the VZ surface. After imaging, these daughters were found to be positive for Sox2 and negative for both Tbr2 and Olig2, suggesting oRG identity. This range in fiber orientation and MST direction has recently been documented in the embryonic macaque cortex (Betizeau et al., 2013), suggesting that this diversity could be a general feature of oRGs.

Because ferret oRGs did not always possess a basally oriented fiber (Figure 3C-E), the fiber along which the progenitor translocated during MST was referred to as the primary (1′) fiber. Although oRGs exhibited variation in division angle with respect to the VZ surface, 96% of MST divisions in the ISVZ and 99% of MST divisions in the OSVZ had a division angle that was perpendicular (60-90°) to the 1′ fiber (Figure 3B). These data are consistent with oRG divisions in human cortical slices and in dissociated human fetal cortex, further supporting the role of intrinsic mechanisms regulating 1′ fiber inheritance and spindle orientation (LaMonica et al., 2013).

Ferret oRG fibers are dynamic and do not always contact the pial surface

Similar to vRGs, data in mouse, human, and ferret suggest that the 1′ fiber of oRGs maintains contact with the basal lamina throughout the cell cycle and exhibits varicosities during M phase (Fietz et al., 2010; Hansen et al., 2010; Wang et al., 2011). Although this appeared to be the case for a subset of oRG divisions in the ferret (Figure 1C,D) (Fietz et al., 2010; Reillo and Borrell, 2012), we observed several instances where the 1′ fiber of the oRG completely retracted during mitosis. An example of this is shown in Figure 4A. As the soma of the oRG begins to translocate toward the 1′ fiber, the fiber begins to retract, and is completely retracted at the time of division. Interestingly, the division angle remains perpendicular (60-90°) to the orientation of the original 1′ fiber even though it has retracted. Upon cytokinesis, both the basal and apical daughters exhibit process outgrowths that increase in length over time. In addition to retraction of the 1′ fiber during mitosis, we also observed oRGs that exhibited retraction of a non-1′ fiber. Similar to the human (LaMonica et al., 2013) and macaque (Bayatti et al., 2008), we found examples of ferret oRG cells, which in addition to a 1′ fiber, possessed a non-1′ fiber that varied in length from 8 to 97μm. As seen in Figure 4B, an oRG possesses a non-1′ apical fiber that is retracted during basal MST, after which the apical daughter re-grows an apically directed fiber. These data suggest that maintenance of the 1′ fiber is not required for oRG proliferation, one of the oRG daughters does not always inherit the 1′ fiber, and oRG fibers can exhibit a variety of behaviors during mitosis.

The retraction of the 1′ fiber during MST (Figure 4A), along with the observation of 1′ fibers that are not basally directed (Figure 3C,E), corroborate findings in cultured human fetal cortex that oRGs do not need to be in contact with the basal lamina to divide (LaMonica et al., 2013). Further evidence suggesting that not all oRG fibers contact the pial surface comes from the observation of growth cones and filopodia-like processes at the end of oRG 1′ fibers. These growth cones could be found at the end of 1′ fibers that did not retract during MST (Figure 4C). Similar to descriptions of mouse vRG basal fiber end feet near the pial surface (Yokota et al., 2010), growth cones of oRG 1′ fibers were motile and displayed various morphologies. They also exhibited dynamic behaviors throughout the cell cycle, including retraction at the time of cell division (Figure 4B).

We have identified diverse behaviors of oRG cells in the developing ferret cortex. Many distinguishing features of oRGs to date, including location in the SVZ, MST mode of division, and presence of a basal fiber that is maintained during mitosis, are not features shared by all oRGs.

Human oRGs exhibit diverse behaviors similar to the ferret

Upon observing a range of oRG behaviors in the ferret, we further investigated the developing human cortex to see whether these oRG characteristics were present in primate species. Human cortical slices were labeled with AV-GFP and imaged using time-lapse confocal microscopy. Although we did not observe stationary oRG divisions at gestational week (GW) 17.5-18 (0/71), we found examples of MST divisions occurring within the human VZ. As illustrated in Figure 5A, for example, a RG cell undergoes apically directed interkinetic nuclear migration (INM) to reach the VZ surface and then initiates MST to divide at the basal region of the VZ with a horizontal angle (3°) with respect to the VZ surface. The basal daughter inherits the basal fiber and migrates away from the VZ, whereas the apical daughter remains in the VZ region. Of 57 divisions where the RG cell was located near the VZ surface, eight exhibited MST, with an average length of 76.2μm. Similar to the ferret (Figure 2), all of these MST divisions were at a horizontal angle (0-30°) with respect to the VZ surface. This suggests that in addition to the SVZ, MST divisions in the human can also occur within the VZ.

Human oRGs within the SVZ could be observed undergoing non-basally directed MST and dividing with a non-horizontal angle with respect to the VZ surface. Surprisingly, we found that 9.9% of human MST divisions in the SVZ at GW 17.5-18 were apically directed. Due to the thickness of the human cortex at this age, it was not possible to measure oRG division angle with respect to the VZ surface. Therefore, we measured oRG division angle with respect to the adjacent radial fiber scaffold and found that the majority of oRGs (77%) divided at a perpendicular angle (60-90°), while 20% and

3% divided at an oblique (30-60°) and parallel (0-30°) angle, respectively (Figure 5B). An example of an oRG dividing with a non-perpendicular cleavage angle with respect to the radial fiber scaffold is shown in Figure 5C. Because the VZ surface in primates is approximately at right angles relative to the radial fiber scaffold (Rakic, 1971), we concluded that the majority of oRGs (77%) in the human SVZ divide with a horizontal angle with respect to the VZ surface, whereas fewer divide with an oblique (20%) and vertical angle (3%). Only 23% of human oRGs divided non-horizontally with respect to the VZ surface, compared with an average of 43% of ferret oRGs, suggesting that ferret oRGs display a greater variation in division angle, which could be the result of 1′ oRG fibers in the ferret being less radial compared with the human.

Similar to the ferret, the 1′ fiber of human oRGs does not always contact the pial surface. As seen in Figure 5D, we observed oRG divisions in which the 1′ fiber fully retracted during mitosis and then re-grew after cytokinesis. We also observed growth cones at the end of oRG 1′ fibers located within the SVZ. Similar to the ferret, these growth cones could be found on the end of 1′ fibers that did not retract during mitosis (Figure 5E). Together, these data demonstrate that diverse and dynamic oRG behaviors are not unique to the ferret and can also be found in the developing human neocortex.

Daughters of ferret oRGs undergo multiple rounds of divisions and remain undifferentiated

We next examined the proliferative capacity and daughter cell fates of ferret oRGs. Similar to the human (Hansen et al., 2010), both oRG daughters were able to undergo multiple rounds of division. The "basal" daughter of an MST division, which either inherited the 1′ fiber or re-grew one upon retraction (Figure 3A), was referred to as the primary (1′) daughter. The "apical" daughter of an MST division that did not inherit the 1′ fiber was referred to as the non-primary (non-1′) daughter. The 1′ and non-1′ daughters had an average cell cycle length of 26.4 h (n=10) and 25.5 h (n=10), respectively. Of 11 examples where the 1′ daughter of an oRG divided a second time, four exhibited a second MST division that was increased in length compared with the initial MST (Figure 6A), four exhibited a second MST division that was decreased in length compared with the initial MST, and three underwent a second division that was stationary (Figure 6B). Interestingly, in 3/11 examples, the oRG daughter migrated basally >100μm before undergoing a subsequent division (Figure 6A). We observed three consecutive MST divisions by a 1′ oRG daughter; however, limitations of slice culture prevented further cell cycles from being observed (Movie 3). We also documented 11 examples where the non-1′ daughter of an oRG divided a second time. Of these, four exhibited a second MST division that ranged in length from 6.3 to 17.9μm, with two of these being a greater distance compared with the initial MST (Figure 6C). The remaining seven underwent a second division that was stationary (Figure 6D).

These data suggest that fiber inheritance is not required for maintenance of proliferative capacity, and that although both oRG daughters can persist as progenitors, the 1′ daughter appears more likely to undergo a second MST division (8/11) compared with the non-1′ daughter (4/11). Some oRG daughters may have become committed progenitors, such as IPCs or glial progenitors, both of which do not appear to exhibit MST. However, because not all ferret oRGs undergo MST (Figure 1D), it is also possible that both daughters remained oRGs. Fate staining after time-lapse imaging was used to address these possibilities.

All fate-stained oRG 1′ (closed white arrowheads, 37/37) and non-1′ daughters (closed yellow arrowheads, 34/34) continued to express the neural progenitor marker Sox2, although none expressed the upper layer neuronal marker Satb2 (0/20) (Figure 7A), or the early neuronal marker HuC/D (0/12, data not shown). Although we observed oRG daughters migrating radially (Figure 7A), a behavior reminiscent of newborn neurons, ferret oRGs do not appear to make neurons directly. To determine the types of progenitors produced by ferret oRGs, slices were stained for Tbr2 and Olig2, IPC and oligodendrocyte progenitor markers, respectively, following time-lapse imaging. Because astrocytes do not appear within the SVZ until P6 or later (Reillo and Borrell, 2012), we did not fate stain for this lineage. None of the oRG daughters expressed Olig2 (0/31) (Figure 7B). Only 1 of 22 1′ oRG daughters and 1 of 20 non-1′ oRG daughters expressed Tbr2 (Figure 7B). Similar results were obtained for the daughters of stationary oRG divisions in which the 1′ fiber was basally directed and did not retract during mitosis. Specifically, both daughters expressed Sox2 (8/8), while none expressed Olig2 (0/8) or Tbr2 (0/6) (Figure 7C).

oRG cells may undergo multiple self-renewing divisions before producing differentiated progenitors and/or the onset of Tbr2 and Olig2 expression may require longer times in culture. Therefore, we stained oRG daughters that had undergone multiple rounds of division. After two rounds of division, daughters expressed Sox2 (20/20) but not Tbr2 (0/12) or Olig2 (0/12). It is also possible that oRGs produce differentiated cells only at earlier stages of neurogenesis. Therefore, we analyzed the marker expression profile of daughters produced by oRGs at E39, which corresponds to the peak of layer IV production. All of the E39 oRG daughters expressed Sox2 (25/25), while only 1 of 25 expressed Tbr2, and none expressed Olig2 (0/25) (Figure 7D).

Together, these results suggest that ferret oRGs undergo several rounds of proliferative divisions to expand the progenitor population, do not give rise to postmitotic neurons or glial progenitors directly, and have the ability to produce neuronal progenitors.

Discussion

Although we are only beginning to uncover mechanisms contributing to the evolutionary expansion and gyrification of the mammalian cortex, recent studies have focused on the contribution of embryonic germinal zones. Specifically, the SVZ is expanded in gyrencephalic species and contains the newly characterized oRG cells, which in addition to IPCs, contribute to neurogenesis in mouse and human (Lui et al., 2011). However, there is not a direct association between SVZ size and oRG abundance with degree of gyrification. Specifically, the lissencephalic mouse has a modest population of oRGs (Shitamukai et al., 2011; Wang et al., 2011), whereas the near-lissencephalic marmoset has an expanded SVZ with abundant oRGs (Garcia-Moreno et al., 2012; Kelava et al., 2012). Although oRG numbers do not predict cortical topography, it is possible that their dynamic behaviors, including proliferative potential and daughter identities, help determine adult cortical structure. Therefore, it is important to assess these features in a range of gyrencephalic and lissencephalic species.

In the present study, we used time-lapse imaging to analyze progenitor behaviors in the ferret, a gyrencephalic carnivore with an expanded SVZ. We found that during upper layer cortical neurogenesis, a third of SVZ divisions exhibit MST, a mode of division that was first identified in the human and is unique to oRG progenitors (Hansen et al., 2010). Mean MST length in the human cortex (Hansen et al., 2010) was nearly three times as large as in the ferret. We also observed several oRG-like divisions, where the basal fiber was maintained during mitosis and inherited by the basal daughter, but which lacked a distinct MST, suggesting that ferret oRGs can undergo stationary divisions. It would be interesting to determine the prevalence of stationary divisions in other species, and to address variations in MST length as a function of age.

Originally, oRGs were described in the OSVZ, but they are now known to exist in the mouse, a species that lacks an elaborate OSVZ, and in the ISVZ and OSVZ of the ferret and marmoset (Garcia-Moreno et al., 2012; Kelava et al., 2012; Reillo and Borrell, 2012). We found that the majority of ferret MST divisions occur within the ISVZ, with oRGs dividing closer to the VZ surface tending to exhibit greater MST lengths. However, static marker expression analyses in the ferret predict that a larger percentage of oRGs reside in the OSVZ compared with the ISVZ (Reillo and Borrell, 2012). Therefore, our data suggest that oRGs located within the OSVZ have a greater tendency to undergo stationary divisions. Interestingly, ~7% of ferret MST divisions observed occurred within the VZ region. This is in agreement with a recent study, in which subapically dividing RGs in the ventral telencephalon of the mouse exhibited MST (Pilz et al., 2013), suggesting that oRG divisions can occur in all three proliferative zones.

In both human and mouse, vRGs have been shown to produce oRGs via horizontal divisions (LaMonica et al., 2013; Shitamukai et al., 2011; Wang et al., 2011). According to fixed image analyses in the ferret, the majority of VZ divisions at P6 are horizontal, suggesting a significant production of oRGs (Chenn and McConnell, 1995; Reillo and Borrell, 2012). Our time-lapse data corroborate these findings as the vast majority of vRG divisions were at an oblique (30-60°) or horizontal (0-30°) angle and produced a basal daughter that inherited the basal fiber, migrated away from the VZ surface, and expressed Sox2, indicative of oRG fate. Surprisingly, in both the ferret and human we observed RG cells at the VZ surface that underwent MST and divided with a horizontal angle to produce a basal daughter with oRG characteristics. Although it is possible that oRGs generated from vRGs remain within the VZ where they divide via MST, INM often preceded MST divisions at the VZ surface. Therefore, it is likely that vRGs can become untethered from the apical domain and undergo MST to produce a basal oRG daughter. Whether the apical daughter of such an MST division is able to anchor within the adherens junction belt and assume a vRG identity or remains delaminated from the VZ surface is unknown. These data further support a close relationship between vRGs and oRGs, and suggest that association with adherens junctions may determine whether RG cells divide via INM or MST.

In our time-lapse analysis of ferret MST divisions, 43% exhibited a non-horizontal division angle relative to the VZ surface. This is in contrast to the primate, where only 23% of oRG divisions in the human and ~20% in the macaque (Betizeau et al., 2013) were non-horizontal. The primate has a predominantly straight radial fiber scaffold running through the SVZ to the cortical plate, whereas the ferret has a more fanned array of radial fibers (Borrell and Reillo, 2012; Reillo et al., 2011). Ferret oRG fibers may exhibit greater curvature and less radial orientation causing more variable division angles as the cell translocates along the fiber during mitosis. This may also contribute to the greater tangential dispersion of clonally related neurons that has been described in the ferret (Reid et al., 1997) compared to the primate cortex (Kornack and Rakic, 1995), resulting in species differences in cortical organization. Despite this variation, ferret oRGs consistently divide at a perpendicular angle with respect to the primary fiber (along which the cell translocates), which is in agreement with recent data from both dissociated cultures and slices of human cortex (LaMonica et al., 2013). The primary fibers of oRG cells do not always contact the pial surface, and some retract during mitosis, suggesting that similar to vRGs (Haubst et al., 2006), contact with the basal lamina is not required for oRG proliferation. However, possible regulation of oRGs by signals from other sources, such as neighboring cells and blood vessels, remains unknown.

Human oRGs undergo multiple rounds of self-renewing divisions with the basal daughter maintaining oRG identity and the apical daughter adopting IPC or oRG fate (Hansen et al., 2010). Similar to the human, we found that ferret oRGs undergo multiple rounds of divisions, with 73% of basal (primary) daughters and 36% of apical (non-primary) daughters dividing via MST in the subsequent division. Because not all ferret oRGs exhibit MST, some of the apical oRG daughters that underwent stationary divisions may have nonetheless adopted oRG fate. This interpretation is supported by fate-staining analysis, as the vast majority of oRG daughters expressed Sox2 but not Satb2, HuC/D, Olig2, or Tbr2. Therefore, oRGs that exhibit stationary divisions and whose primary fiber does not contact the pial surface are likely oRG apical daughters that adopted oRG fate. Together, these results suggest that ferret oRGs exhibit similar proliferative potential to human oRGs; however, they appear to produce IPCs less frequently (Hansen et al., 2010) (Table 1).

These data highlight diversity within the ferret and human oRG populations in terms of location, morphology including fiber orientation, and mitotic dynamics (Figure 8). Despite this heterogeneity, oRGs express a common set of markers (Sox2+, Tbr2-, Olig2-), possess a primary fiber, and display a consistent division angle determined by primary fiber orientation. Morphological variation within the oRG population has recently been documented in the macaque cortex (Betizeau et al., 2013) and in the ventral telencephalon of the mouse (Pilz et al., 2013). For example, a subapically dividing bipolar RG cell was described that possesses both an apical and basal process and appears to be more abundant in gyrencephalic species. In this study, we also observed bipolar ferret oRG-like cells; however, we found that both apical and basal fibers could rapidly retract during mitosis, suggesting that oRG morphology can undergo cell cycle-related changes. These rapid morphological changes could have been missed with longer imaging intervals.

It has been proposed that differences in progenitor cell process morphology, as well as variation in the location of dividing progenitor cells, may indicate the existence of multiple progenitor subtypes (Betizeau et al., 2013; Pilz et al., 2013). However, in these studies, cells assigned to distinct subtypes were not identified based on unique molecular marker profiles or mitotic behaviors, and many of the progenitor subtypes described share important features with the initially described oRG cells (Fietz et al., 2010; Hansen et al., 2010). Thus, we propose that many or all of these cells belong to a broad progenitor class. Individual cells within this class may transition between locations and phenotypic states, and exhibit differences in proliferative capacity and daughter output as they age. Single cell gene expression studies may enable a more accurate subclassification of the SVZ progenitor populations, linking molecular signatures to progenitor cell location, morphology, and/or behavior.

Figure 1. SVZ divisions in the developing ferret cortex.

(A) P3 ferret cortical slice labeled with AV-GFP and stained for Sox2 (blue), Tbr2 (red), and Olig2 (white) to distinguish the VZ (100µm thick on average) from the iSVZ (150µm thick on average) and oSVZ (400µm thick on average). Boxed region indicates the location of the magnified region, which highlights AV-GFP+ cells within the iSVZ and oSVZ that are Sox2+, Tbr2-, and Olig2- (white closed arrowheads). Scale bars: in merged image, 50µm; in single channel images, 20µm. (B) Box plot showing median and interquartile range of MST distances in the iSVZ and oSVZ (n=162). (C, D) Time-lapse stills of oRGs labeled with AV-GFP in P3 ferret cortical slices. Time elapsed from start of imaging indicated in top right of image (hours:minutes, yellow = start of division). VZ surface is down. Scale bars, 20µm. (C) An oRG (closed white arrowhead) maintains the basal fiber (open white arrowheads) during mitosis and exhibits an MST length of 37µm (white arrow indicates direction of MST) to produce a basal (closed white arrowhead) and apical daughter (closed yellow arrowhead). (D) An example of a stationary oRG division in which the cell (closed white arrowhead) maintains the basal fiber (open white arrowheads) during mitosis, and produces a basal (closed white arrowhead) and apical daughter (closed yellow arrowhead).

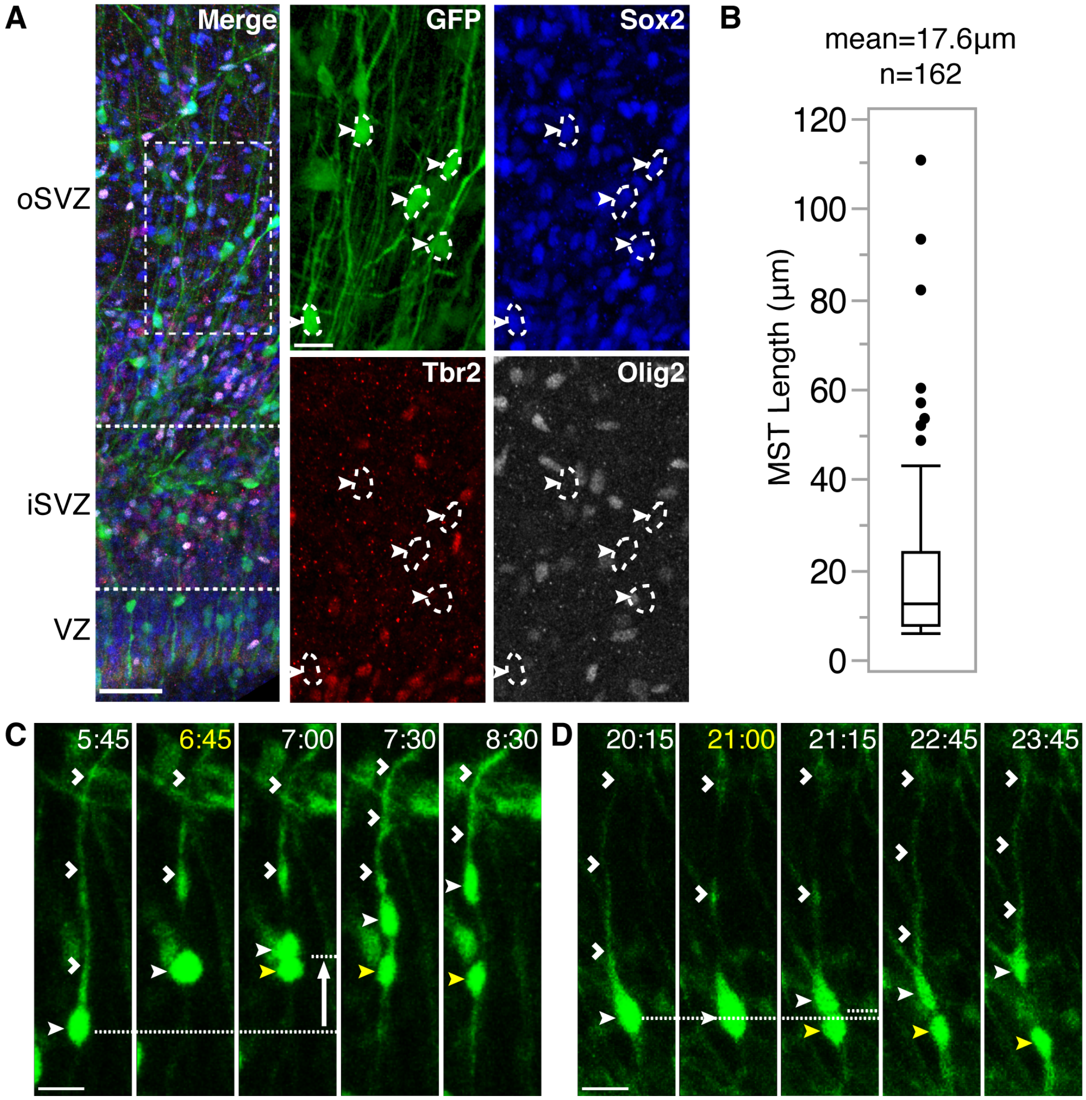
A
Merge
GFP
Sox2
Tbr2
Olig2
oSVZ
iSVZ
VZ
B
mean=17.6µm
n=162
MST Length (µm)
0
20
40
60
80
100
120
C
5:45
6:45
7:00
7:30
8:30
D
20:15
21:00
21:15
22:45
23:45

Figure 2. MST divisions can be found throughout the VZ and SVZ.

(A) Percentage of SVZ MST divisions (n=162) occurring at different distances from the VZ surface (100-650μm). (B) Scatter plot and linear regression line were used to analyze the relationship between MST length and division location measured as distance from the VZ surface (n=174). The regression line equation is $y = 23.585-0.0199x$; $r^2 = 0.0296$, $p = 0.023$ (*$p<0.05$). (C, D) Time-lapse stills of RG cells labeled with AV-GFP in P3 ferret cortical slices. Time elapsed from start of imaging indicated in top right of image (yellow = division). VZ surface is denoted by a dotted line. Basal daughter indicated with closed white arrowhead and apical daughter with closed yellow arrowhead. Boxed region indicates the location of the basal daughter at the end of time-lapse imaging. Scale bars, 20μm. (C) An RG (closed white arrowhead) divides at the VZ surface with an oblique division angle (36.7° with respect to VZ surface) to produce a basal daughter that inherits the basal process (open white arrowheads) and an apical daughter. Post-time-lapse fate staining reveals that the basal daughter is Sox2+. Shown on the right is a schematic of the time-lapse series. (D) An RG (closed white arrowhead) located at the VZ surface undergoes basal MST (10.9μm, white arrow indicates direction of MST) and divides with a horizontal division angle (4.4° with respect to VZ surface) to produce a basal daughter that inherits the basal process (open white arrowheads) and an apical daughter. Post-time-lapse fate staining reveals that the basal daughter is Sox2+. Schematic of time-lapse series is shown on the right.

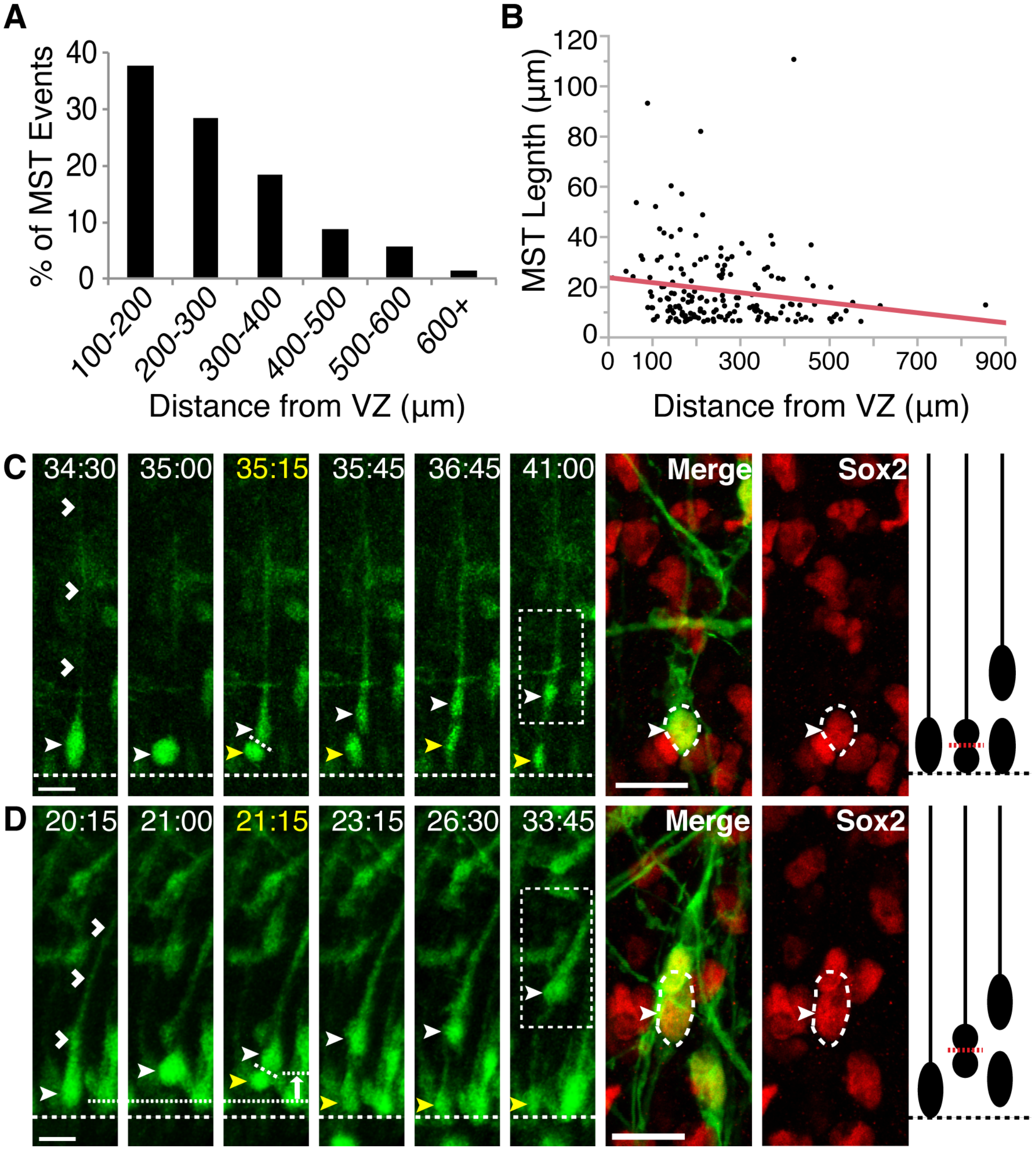
A
% of MST Events
40
30
20
10
0
100-200
200-300
300-400
400-500
500-600
600+
Distance from VZ (µm)
B
MST Legnth (µm)
120
100
80
60
40
20
0
0
100
300
500
700
900
Distance from VZ (µm)
C
34:30
35:00
35:15
35:45
36:45
41:00
Merge
Sox2
D
20:15
21:00
21:15
23:15
26:30
33:45
Merge
Sox2

Figure 3. oRG division angles vary with respect to the VZ surface but remain constant with respect to the primary fiber.

(A) Schematic and quantification of cells undergoing MST with horizontal (0-30°, blue), oblique (30-60°, red), and vertical (60-90°, green) division angles with respect to the VZ surface (n=174). (B) Schematic and quantification of cells undergoing MST with vertical (0-30°, green), oblique (30-60°, red), and horizontal (60-90°, blue) division angles with respect to the primary (1′) fiber (n=174). (C - E) Time-lapse stills of progenitors labeled with AV-GFP in P3 ferret cortical slices. Time elapsed from start of imaging indicated in top right of image (yellow = division). 1′ daughter is denoted with a closed white arrowhead and non-1′ daughter with a closed yellow arrowhead. Yellow line indicates 1′ fiber orientation prior to MST. White arrow indicates the direction of MST. VZ surface is down. Scale bars, 20μm. (C) An oRG (closed white arrowhead) undergoes MST (17.1μm, 100.6μm from VZ surface) to produce daughters that are Sox+Tbr2-Olig2-, and that possess 1′ fibers (open white arrowheads) that are parallel to the VZ surface. (D) Example of a progenitor undergoing MST (16μm, 100μm from VZ surface) parallel to the VZ surface and dividing 86° relative to the 1′ fiber (open white arrowheads). (E) Example of a progenitor undergoing apically directed MST (33μm, 320μm from VZ surface) and dividing 76° relative to the 1′ fiber (open white arrowheads).

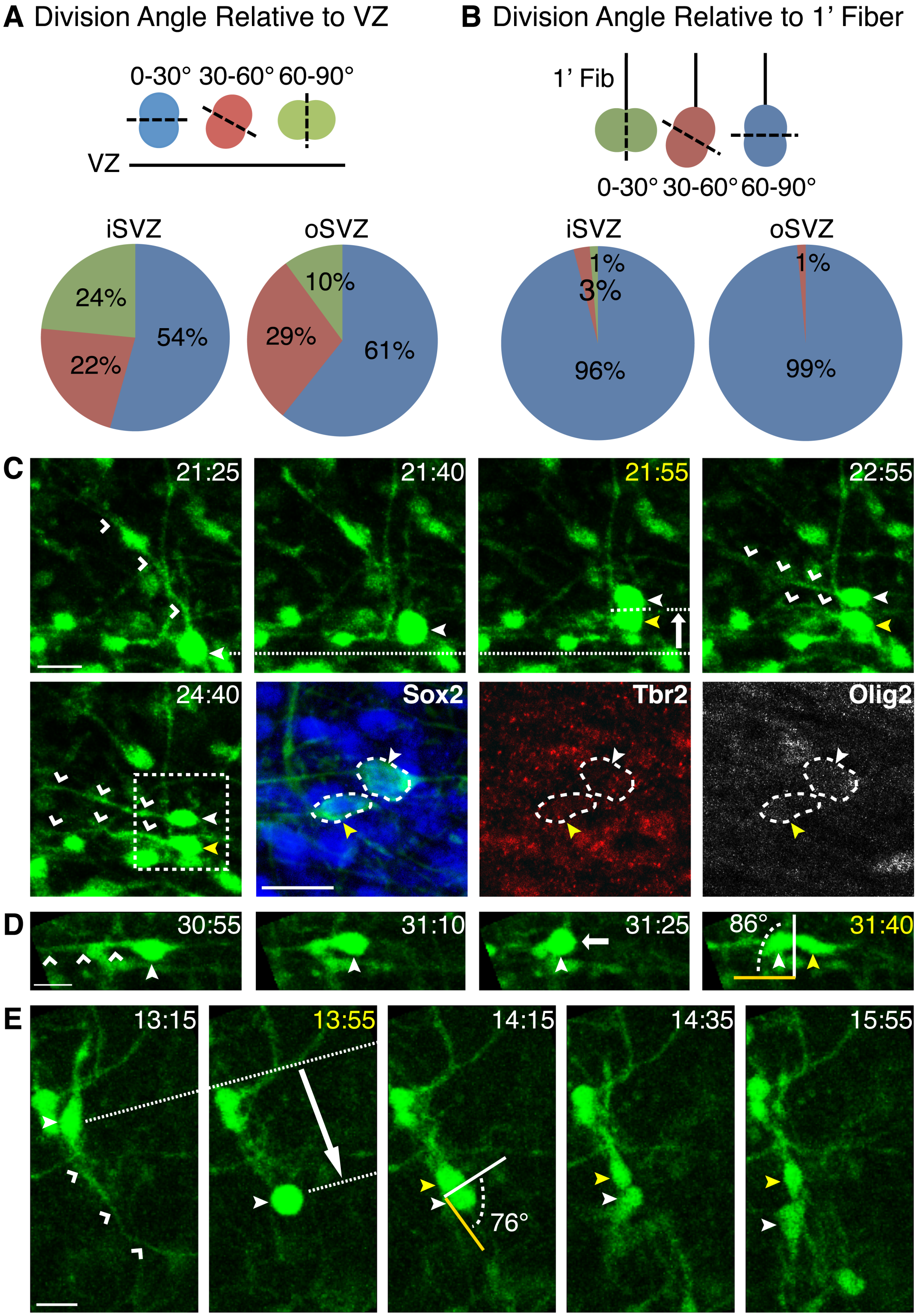
A Division Angle Relative to VZ
0-30°
30-60°
60-90°
VZ
iSVZ
24%
54%
22%
oSVZ
10%
29%
61%
B Division Angle Relative to 1' Fiber
1' Fib
0-30°
30-60°
60-90°
iSVZ
1%
3%
96%
oSVZ
1%
99%
C
21:25
21:40
21:55
22:55
24:40
Sox2
Tbr2
Olig2
D
30:55
31:10
31:25
86°
31:40
E
13:15
13:55
14:15
76°
14:35
15:55

Figure 4. oRG fibers are dynamic during the cell cycle and do not always contact the pial surface.

Time-lapse stills of progenitors labeled with AV-GFP in P3 ferret cortical slices. Time elapsed from start of imaging indicated in top right of image (yellow = division). Basal daughter indicated with closed white arrowhead and apical daughter with closed yellow arrowhead. White arrow indicates the direction of MST. VZ surface is down. Scale bars, 20µm. (A) An oRG (closed white arrowhead, 281µm from VZ surface) exhibits retraction of the basal, 1′ fiber (open white arrowheads, 125.8µm) during MST (32µm), which then re-grows after cytokinesis. A corresponding z-plane analysis of the same time point rotated 90° confirms retraction of the 1′ fiber during mitosis. (B) An oRG (closed white arrowhead, 476.7µm from VZ surface) possesses an apical, non-1′ fiber (open white arrowheads, 62µm) that retracts during MST (18.3µm). A corresponding z-plane analysis rotated 90° confirms retraction of the apical fiber during mitosis. (C) An oRG (closed white arrowhead, 149µm from VZ surface) with a basally directed 1′ fiber measuring 297µm (open white arrowheads) maintains the fiber during MST (9.5µm). Top, A zoomed-in view of the end of the 1′ fiber revealing a growth cone that is motile and dynamic during the cell cycle.

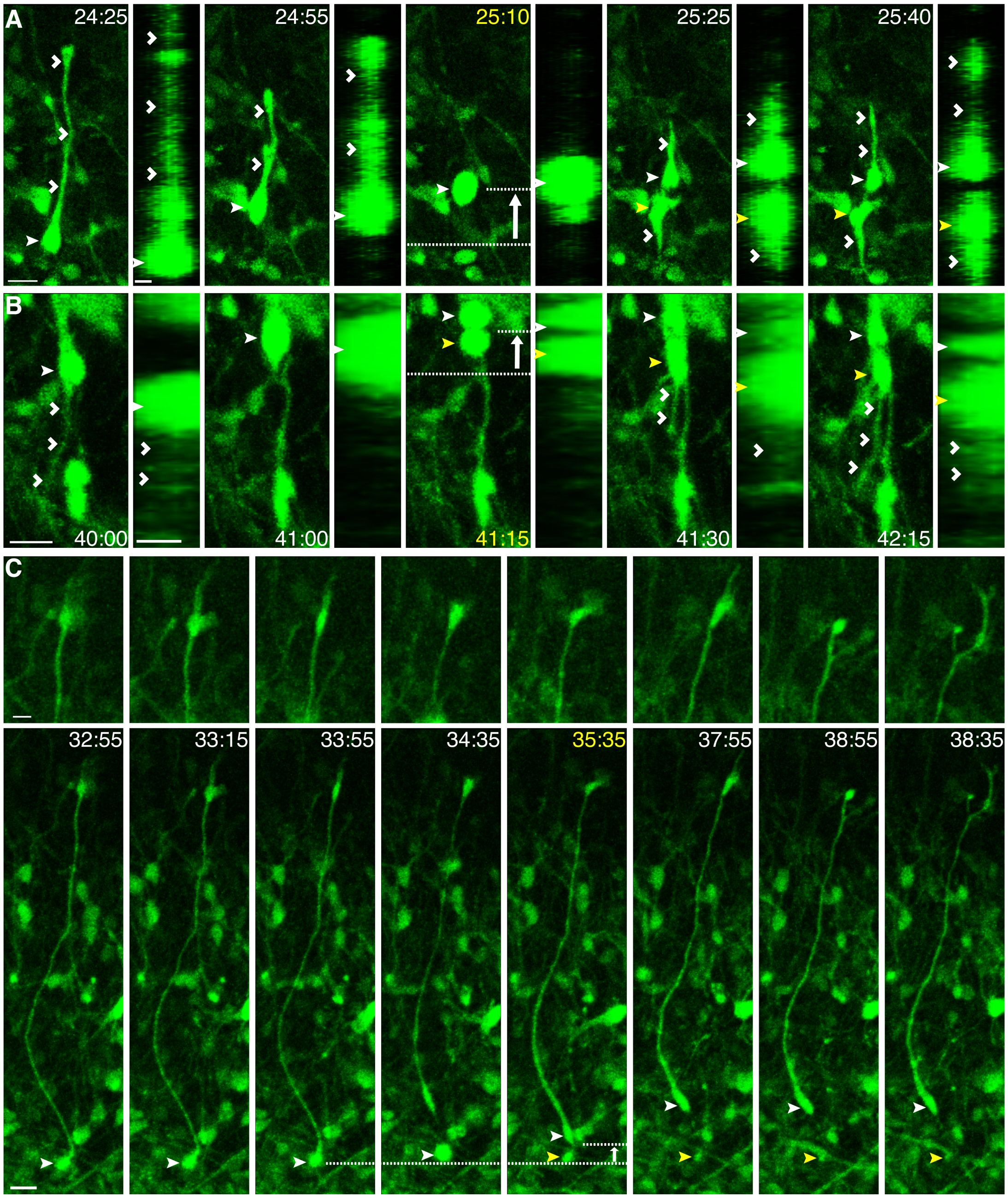
A
24:25
24:55
25:10
25:25
25:40
B
40:00
41:00
41:15
41:30
42:15
C
32:55
33:15
33:55
34:35
35:35
37:55
38:55
38:35

Figure 5. Human oRGs exhibit diverse behaviors similar to the ferret.

Time-lapse stills of progenitors labeled with AV-GFP in human cortical slices from GW 16 (A) and 18 (C - E). Time elapsed from start of imaging indicated in top right of image (yellow = division). White arrow indicates the direction of MST. VZ surface is down and denoted by a dotted line. Scale bars, 20μm. (A) A vRG (closed white arrowhead) undergoes INM to reach the VZ surface followed by basal MST (64μm), dividing with a horizontal division angle (3° with respect to VZ surface) to produce a basal (closed white arrowhead) and apical daughter (closed yellow arrowhead). Schematic of time-lapse series in is shown on the right. (B) Schematic and quantification of cells undergoing MST with horizontal (0-30°, green), oblique (30-60°, red), and vertical (60-90°, blue) division angles with respect to the adjacent fiber scaffold (n=71). (C) A progenitor (open white arrowhead) undergoes MST (29μm) and divides with a 30° angle with respect to the radial fiber scaffold (yellow line). (D) An oRG (closed white arrowhead) displays retraction of the 1′ fiber (open white arrowheads, 103.7μm) during MST (37.2μm) after which daughters (closed white and yellow arrowheads) re-grow fibers (open white arrowheads). A corresponding z-plane analysis rotated 90° confirms retraction of the 1′ fiber during mitosis. (E) An oRG (closed white arrowhead) has a basally directed 1′ fiber (open white arrowheads, 202.7μm) that ends in a growth cone that is motile and dynamic during MST (125μm). Top, A zoomed-in view of the growth cone.

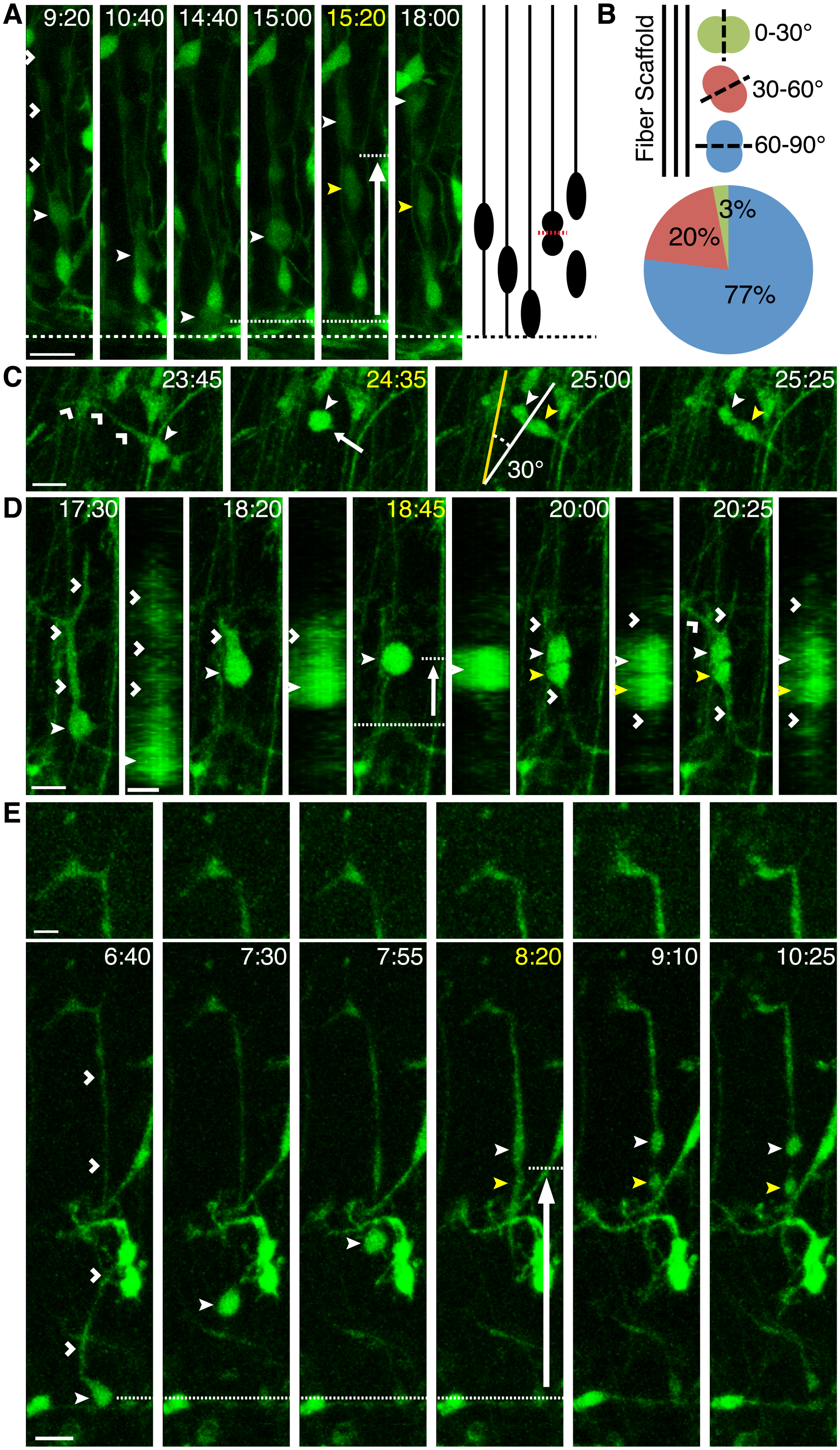
A
9:20
10:40
14:40
15:00
15:20
18:00
B
Fiber Scaffold
0-30°
30-60°
60-90°
3%
20%
77%
C
23:45
24:35
25:00
30°
25:25
D
17:30
18:20
18:45
20:00
20:25
E
6:40
7:30
7:55
8:20
9:10
10:25

Figure 6. oRG daughters can undergo multiple rounds of divisions.

Time-lapse stills of progenitors labeled with AV-GFP in P3 ferret cortical slices along with schematics illustrating the divisions shown in the time-lapse series (D = daughter). Time elapsed from start of imaging indicated in top right of image (yellow = division). White arrow indicates direction of MST. VZ surface is down. Scale bars, 20µm. (A) The 1′ daughter from an MST division (18µm) during which the 1′ fiber is retracted (open white arrowheads), migrates basally (105µm) and undergoes a second MST division (25µm) with fiber retraction. (B) The 1′ daughter (closed white arrowhead) of an MST division (28µm), during which the 1′ fiber is retracted (open white arrowheads), undergoes a second stationary division where the 1′ fiber is maintained (open white arrowheads). (C) The non-1′ daughter (closed yellow arrowhead) of an MST division (13µm), during which the 1′ fiber is retracted (open white arrowheads), re-grows a basal fiber (open white arrowheads), and undergoes a second MST division (18µm) with apparent fiber retraction. (D) The non-1′ daughter (closed yellow arrowhead) of an MST division (32µm), during which the 1′ fiber is retracted (open white arrowheads), re-grows a basal fiber, and undergoes a second stationary division where the 1′ fiber is maintained (open white arrowheads).

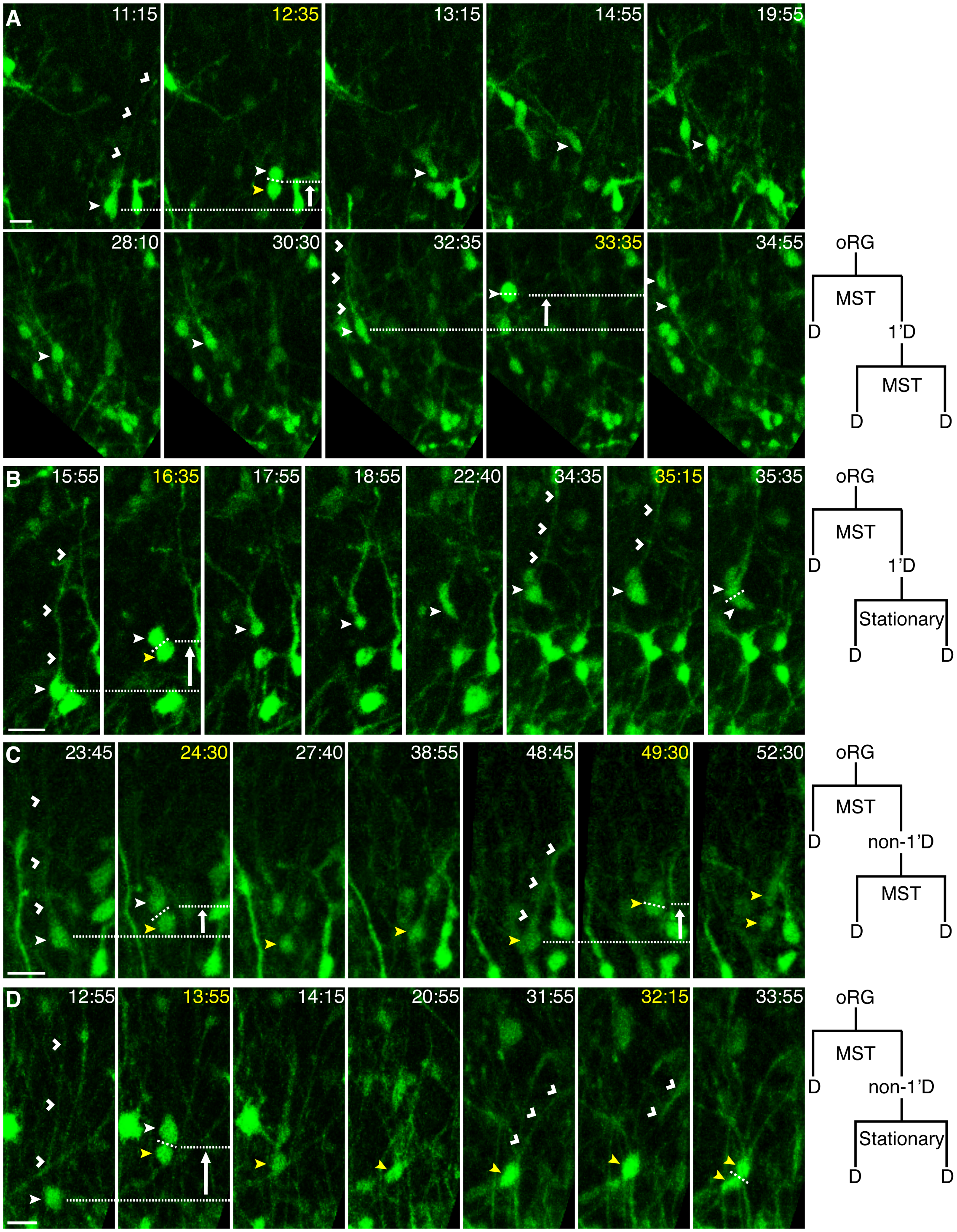
A
11:15
12:35
13:15
14:55
19:55
28:10
30:30
32:35
33:35
34:55
oRG
MST
D
1'D
MST
D
D
B
15:55
16:35
17:55
18:55
22:40
34:35
35:15
35:35
oRG
MST
D
1'D
Stationary
D
D
C
23:45
24:30
27:40
38:55
48:45
49:30
52:30
oRG
MST
D
non-1'D
MST
D
D
D
12:55
13:55
14:15
20:55
31:55
32:15
33:55
oRG
MST
D
non-1'D
Stationary
D
D

Figure 7. The majority of oRG daughters remain undifferentiated.

Time-lapse stills of progenitors labeled with AV-GFP in P3 (A - C) or E39 (D) ferret cortical slices. Time elapsed from start of imaging indicated in the top right of image (yellow = division), with fate stains performed at 66:50 (A - C) or 50:00 (D). 1′ fiber indicated with open white arrowheads. White arrow indicates the direction of MST. Basal (1′) daughter indicated with closed white arrowhead and apical (non-1′) daughter with closed yellow arrowhead. VZ surface is down. Scale bars, 20μm. (A) An oRG (closed white arrowhead) undergoes MST (68μm) to produce a basal and apical daughter. Boxed regions indicate the location of the daughters at the end of time-lapse imaging. Fate staining reveals that both GFP+ daughters are Sox2+Satb2-. (B) An oRG (closed white arrowhead) undergoes MST (11.2μm) to produce a basal and apical daughter. Boxed region indicates the location of the daughters at the end of time-lapse imaging. Fate staining reveals that both GFP+ daughters are Sox2+Tbr2-Olig2-. (C) An oRG (closed white arrowhead) undergoes a stationary division to produce a basal and apical daughter. Fate staining reveals that GFP+ progeny are Sox2+Tbr2-Olig2-. (D) An oRG (closed white arrowhead) undergoes MST (12.3μm) to produce a basal and apical daughter. Boxed region indicates the location of the daughters at the end of time-lapse imaging. Fate staining reveals that both GFP+ daughters are Sox2+Tbr2-Olig2-.

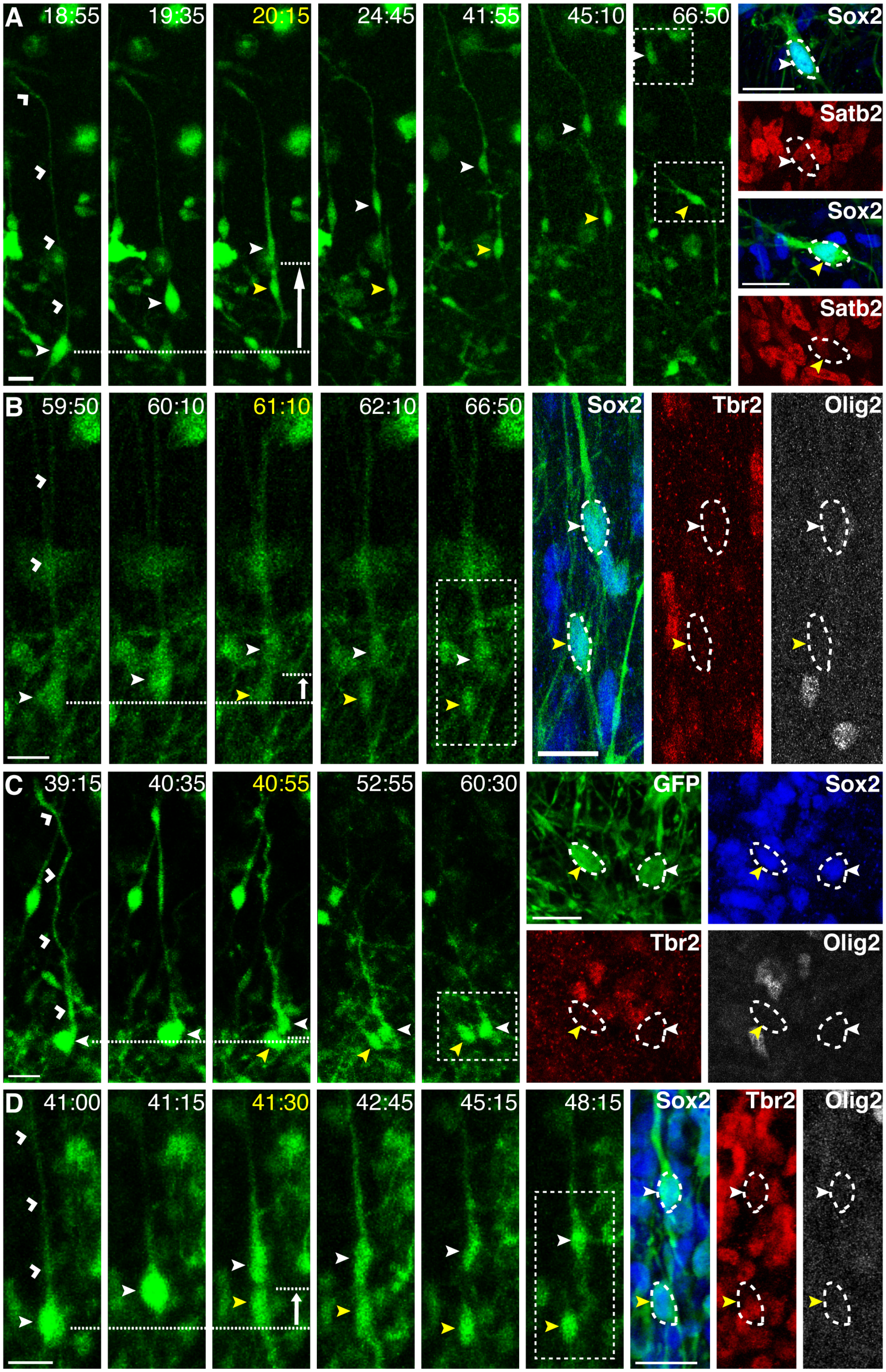
A
18:55
19:35
20:15
24:45
41:55
45:10
66:50
Sox2
Satb2
Sox2
Satb2
B
59:50
60:10
61:10
62:10
66:50
Sox2
Tbr2
Olig2
C
39:15
40:35
40:55
52:55
60:30
GFP
Sox2
Tbr2
Olig2
D
41:00
41:15
41:30
42:45
45:15
48:15
Sox2
Tbr2
Olig2

Figure 8. Model of diverse oRG behaviors and daughter cell fates during cortical development.

*(*A) During neurogenesis in both the ferret and human, MST divisions can occur throughout the VZ and the SVZ and oRGs exhibit diverse morphologies. Specifically, 1′ fibers do not always contact the pial surface, with some ending in motile growth cones within the SVZ. Moreover, not all oRG 1′ fibers are basally oriented, with some exhibiting curved, horizontal, and apical orientations. However, the vast majority of oRGs divide with a perpendicular division angle with respect to the 1′ fiber. (B) The mitotic behavior of oRGs also varies. Although some divide via MST, a subset of oRGs undergoes stationary divisions. In addition, although some oRGs maintain their 1′ fiber during mitosis, which displays varicosities during M phase, some oRGs exhibit retraction of the 1′ fiber upon division. (C) oRGs in different species can produce daughters with different cell fates. In the lissencephalic mouse, oRGs appear to make neurons directly. In the gyrencephalic ferret, the majority of oRGs undergo divisions to expand the oRG population, while a small percentage of oRGs produce IPCs. Compared with the ferret, human oRGs appear more likely to produce IPCs that divide symmetrically to produce neurons, and also undergo proliferative, oRG-producing divisions.

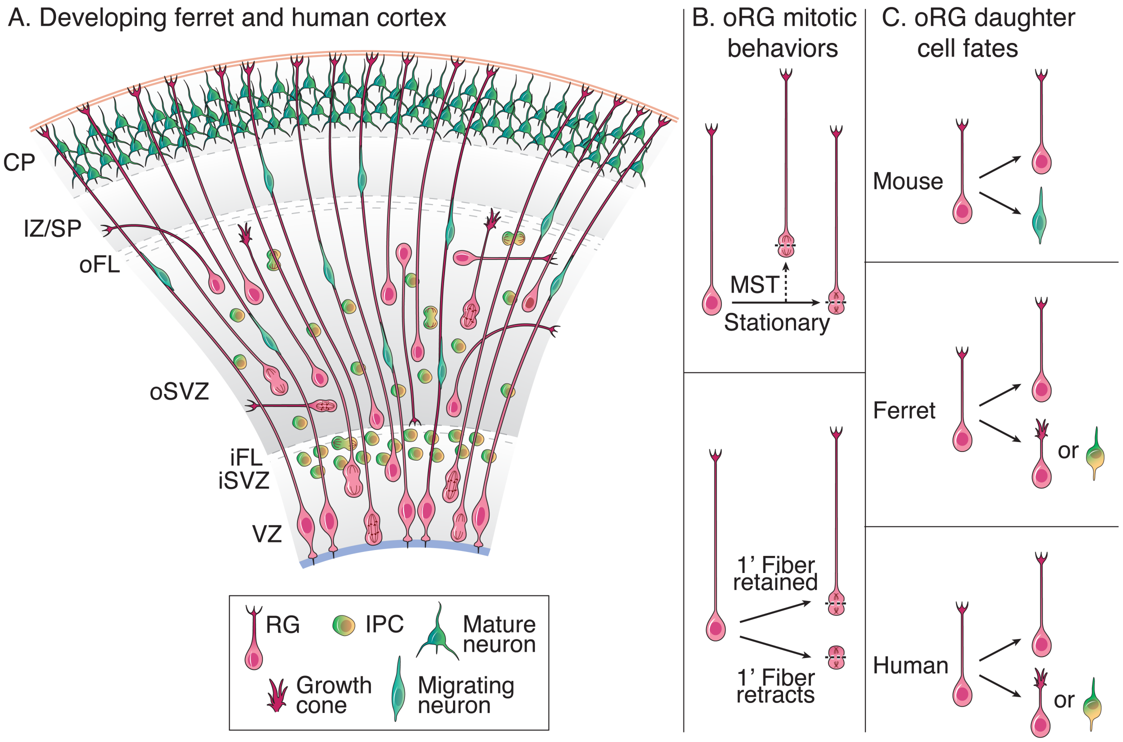
A. Developing ferret and human cortex
CP
IZ/SP
oFL
oSVZ
iFL
iSVZ
VZ
RG
IPC
Mature neuron
Growth cone
Migrating neuron
B. oRG mitotic behaviors
MST
Stationary
1' Fiber retained
1' Fiber retracts
C. oRG daughter cell fates
Mouse
Ferret
or
Human
or

Table 1. Comparison of post-time-lapse oRG daughter cell fates between ferret and human.

Human and ferret slices were labeled with AV-GFP, imaged for several days, and then immunohistochemistry performed to determine oRG daughter cell fates. The Sox2+Tbr2- population represents daughters of oRG MST divisions that remained non-neurogenic progenitors, whereas the Sox2+/-Tbr2+ population represents neurogenic IPCs generated from oRG MST divisions.

*Age of cortical slice preparation. Human GW15.5 corresponds to the end of layer V neurogenesis (Hansen et al., 2010), whereas ferret E39 corresponds to the peak of layer IV production, and P3 is the peak of layer II/III neurogenesis.

Comparison of post-time-lapse oRG daughter cell fates between ferret and human.

Species	Age*	Fate Stain	
		Sox2+Tbr2-	**Sox2+/-Tbr2+**
Human	GW15.5	76.5% (13/17)	17.6% (3/17)
Ferret	P3	95.2% (40/42)	4.8% (2/42)
Ferret	E39	96% (24/25)	4% (1/25)

Movie 1. Ferret oRGs undergo MST and stationary divisions.

In this time-lapse series, SVZ progenitors were labeled with AV-GFP in P3 ferret cortical slices. An oRG (yellow circle) with a basally oriented primary fiber divides via MST (12 µm). Next, an oRG (pink circle), with a curved primary fiber that is basally oriented (white arrowheads), maintains the fiber during mitosis and undergoes a stationary division. This oRG cell has a dynamic growth cone at the end of the primary fiber.

This movie can be accessed online at:

http://www.jneurosci.org/content/34/7/2559.long

Movie 2. RG cells within the ferret VZ divide both at the VZ surface and subapically.

In this time-lapse series, VZ progenitors were labeled with AV-GFP in P3 ferret cortical slices. An RG cell (pink circle) undergoes MST (20 µm) and divides at a subapical position with a horizontal angle with respect to the VZ surface. Next, a nearby RG cell (yellow circle) divides at the VZ surface, followed by another RG cell (orange circle) dividing at the VZ surface.

This movie can be accessed online at:

http://www.jneurosci.org/content/34/7/2559.long

Movie 3. Ferret oRGs undergo multiple rounds of self-renewing divisions.

In this time-lapse series, SVZ progenitors were labeled with AV-GFP in P3 ferret cortical slices. An oRG (yellow circle) with a basally oriented primary fiber undergoes MST (49 μm) to produce a 1′ and non-1′ daughter (yellow circles). Shortly thereafter, another oRG (pink circle) with a basally oriented primary fiber undergoes MST (17.2 μm) to produce a 1′ and non-1′ daughter (pink circles). Both 1′ oRG daughters that retained the primary fiber then undergo a second MST division (yellow circle, 10.1 μm; pink circle, 13.2 μm). The basal, 1′ daughters from these second MST divisions then undergo a third MST division (yellow circle, 12 μm; pink circle, 8.9 μm). From the original, first MST divisions, one of the non-1′ oRG daughters undergoes a stationary division (yellow circle), whereas the other non-1′ oRG daughter undergoes a small MST division (pink circle, 6.1 μm).

This movie can be accessed online at:

http://www.jneurosci.org/content/34/7/2559.long

CHAPTER 4:

Neuronal migration dynamics in the developing ferret cortex

Summary

During development of the mammalian neocortex, newborn excitatory and inhibitory neurons must migrate over long distances to reach their terminal position within the cortical plate. In the rodent, excitatory pyramidal neurons are born in the ventricular and subventricular zones of the pallium and migrate radially along radial glia fibers to reach the appropriate cortical layer. Although much less is known about neuronal migration in gyrencephalic species, retroviral studies in the ferret and primate suggest that unlike the rodent, pyramidal neurons do not follow strict radial pathways and instead disperse tangentially. However, the mechanism by which pyramidal neurons laterally disperse within the folded cortex is unknown. In this study, we identified a technique for visualizing neurogenic divisions and neuronal migration in the ferret, a gyrencephalic carnivore. We found that pyramidal neuron migration was predominantly radial and cortical plate-directed at early postnatal ages. In contrast, neurons displayed more tortuous migration with a decreased frequency of cortical plate-directed migration at later stages of neurogenesis when the ferret brain had begun to fold. This was accompanied by neurons migrating sequentially along several different radial glial fibers, providing a mechanism by which pyramidal neurons may disperse tangentially within the folded cortex. These migratory behaviors may be characteristic of neurons in gyrencephalic species, supporting the use of non-rodent model systems for studying neuronal migration disorders.

Introduction

The mammalian neocortex has a complex cytoarchitecture consisting of six horizontals layers, each with a unique composition of neuronal cells types and connections. In order for the proper functioning of the neocortex, which in humans is crucial for higher cognitive processes, neurons must be born in the correct sequence and populate the appropriate cortical layer. This is not an easy task, as excitatory pyramidal neurons and inhibitory interneurons are generated in distinct germinal regions and must migrate over long distances to reach their laminar position within the cortical plate (CP) (Evsyukova et al., 2013; Marin and Rubenstein, 2003).

Decades of work have shaped our current understanding of neuronal specification and migration in the mammalian cortex. According to the prevailing model, pyramidal neurons are descended from radial glia cells (RGs) that reside in the ventricular zone (VZ) and possess fibers that contact both the ventricular and pial surfaces (Miyata et al., 2001; Noctor et al., 2001; Noctor et al., 2002). Excitatory neurons are also generated by intermediate progenitor cells (IPCs), which are RG daughter cells that reside basal to the VZ in the subventricular zone (SVZ) (Haubensak et al., 2004; Noctor et al., 2004). Neurons then migrate radially along RG fibers, often of the parent cell (Noctor et al., 2001), which serve as scaffolds for neuronal migration (Edmondson and Hatten, 1987; Rakic, 1971, 1972). Interneurons are generated in the ganglionic eminences located in the ventral forebrain and migrate even longer distances to reach the CP. They migrate tangentially into the cortex and then transition to radial migration to reach the appropriate layer (Ang et al., 2003; Marin and Rubenstein, 2001; Nadarajah and Parnavelas, 2002).

While this model depicts developmental events in the rodent, much less is known about neuronal production and migration in the gyrencephalic, or folded, cortex. Differences in the development of a smooth and folded brain may alter neuronal migration properties. Specifically, species with a folded cortex have a greatly expanded SVZ (Lukaszewicz et al., 2005; Martinez-Cerdeno et al., 2012; Reillo et al., 2011; Smart et al., 2002), which requires neurons to travel longer distances to reach the appropriate laminar position. In addition, the SVZ has an increased abundance of progenitors, including outer radial glia (oRGs). oRGs share many features with ventricular RGs (vRGs), except that they lack an apical endfoot contacting the ventricular surface (Fietz et al., 2010; Hansen et al., 2010). oRGs likely provide additional guides supporting neuronal migration, thereby increasing the complexity of the migration scaffold (Lui et al., 2011). Additionally, cortical folding begins while neurons are still being generated and migrating to their final positions. Therefore, neurons must decide whether to migrate to, and terminally occupy, a developing gyrus or sulcus, adding further complications to the migratory pathway.

Evidence suggests that neuronal migration in gyrencephalic species deviates from the prevailing model. Specifically, retroviral studies in the ferret (Reid et al., 1997; Ware et al., 1999) and primate (Kornack and Rakic, 1995) revealed substantial lateral dispersion of clonally related neurons, suggesting that pyramidal neurons do not follow strict radial paths. Static and real-time analyses in the ferret have also demonstrated the tangential orientation of migrating cells within the cortex (O'Rourke et al., 1997; O'Rourke et al., 1992; O'Rourke et al., 1995). However, these studies did not distinguish between pyramidal neuron and interneuron migration. Moreover, the mechanism by which pyramidal neurons distribute laterally remains unknown. A comprehensive analysis of neuronal migration in the gyrencephalic cortex may elucidate mechanisms that differ in a smooth versus folded brain. Since several human neurodevelopmental disorders have been attributed to defects in neuronal migration that have proved difficult to reproduce in the lissencephalic rodent brain, these studies are important for understanding changes in migration patterns that are caused by mutations in disease genes (Evsyukova et al., 2013; Ross and Walsh, 2001).

In the current study, we identified a method for visualizing neurogenic divisions and neuronal migration in the ferret, a gyrencephalic carnivore. Using time-lapse imaging, we observed neurogenic divisions and analyzed the migration pathways of over 550 neurons. We found that the majority of pyramidal neurons migrated radially towards the CP at ages when the ferret cortex has not yet developed folds. In contrast, at later ages when the ferret cortex has begun to fold, neurons migrated in more varied directions and displayed increased non-linearity and turning along their migratory routes. Tortuous migration pathways were accompanied by neurons migrating sequentially along several different RG fibers. These behaviors may be characteristic of neurons in a folded cortex and be essential for the tangential dispersion of pyramidal neurons in gyrencephalic species.

Results

AAV2-CAG-GFP labels migrating neurons in the developing ferret cortex

Using time-lapse imaging, our lab has analyzed ventricular (VZ) and subventricular zone (SVZ) progenitor behaviors in the ferret (Gertz et al., 2014) and human cortex (Hansen et al., 2010; LaMonica et al., 2013; Ostrem et al., 2014). In order to label progenitor populations, we infected cortical slices with an adenovirus where GFP is expressed under the control of the CMV promoter (AV-CMV-GFP). While this technique robustly labels progenitors, we rarely observed migrating cells. We suspected that the CMV promoter might not be readily expressed in immature neurons. Therefore, we sought alternative methods to label and visualize migrating neurons. We identified an adeno-associated virus (serotype 2), where GFP is expressed under the control of the CAG promoter (AAV2-CAG-GFP), and found that this construct robustly labeled cells that migrate throughout the ferret cortex. An example of an AAV2-CAG-GFP labeled cell displaying radial migration towards the cortical plate is shown in Figure 1C. Post-time-lapse staining confirmed pyramidal neuron identity, as the GFP-positive cell expressed the upper layer neuronal marker Satb2.

In order to further validate labeling of post-mitotic neurons by AAV2-CAG-GFP, AV-CMV-GFP or AAV2-CAG-GFP was applied to P2/3 ferret cortical slices. The slices were then cultured for 48-72 hours and immunohistochemistry performed. Approximately 85% of AV-CMV-GFP-positive cells expressed the neural stem cell marker Sox2, compared to only 33% of AAV2-CAG-GFP-positive cells. A similar percentage of CMV-GFP and CAG-GFP-positive cells expressed Olig2, an oligodendrocyte marker, while a slightly greater percentage of CMV-GFP-positive cells expressed Tbr2, an intermediate progenitor cell (IPC) marker. Importantly, an average of

42% of AAV2-CAG-GFP-positive cells expressed the upper layer neuronal marker Satb2, compared to only 4% of AAV2-CAG-GFP-positive cells (Figure 1A and B). This static marker expression data corroborated the time-lapse imaging findings that AV-CMV-GFP preferentially labels ferret neural progenitors, while AAV2-CAG-GFP labels post-mitotic neurons.

Populations of slow and fast neurons migrate within the developing ferret cortex

Using AAV2-CAG-GFP to visualize migrating neurons in the ferret cortex, we performed a comprehensive characterization of neuronal migration at two developmental ages. We analyzed migrating cells at P2 to P3 (P2/3), when the SVZ is expanded and can be divided into an inner and outer region but the cortex has not yet begun to fold. We also analyzed cells at P6 to P7 (P6/7), when the cortex has begun to develop gyri and sulci (Reillo and Borrell, 2012; Smart and McSherry, 1986a, b). At both of these ages, upper-layer projection neurons are being generated (Jackson et al., 1989; McConnell, 1988).

At P2/3, the average migration speed was 11.9 μm/hr (n = 277 with average track duration of 27.6 h), while at P6/7 the average migration speed was 17.9 μm/hr (n = 302 with average track duration of 30.3 h). The vast majority of cells had average track speeds between 4-20 μm/hr, which is comparable to the speed of pyramidal neuron migration previously reported in the rodent (Nadarajah et al., 2001; Takahashi et al., 1996) and ferret (O'Rourke et al., 1997; O'Rourke et al., 1992) (Figure 2B). Due to deviations of the z-axis during imaging, migration distances were only measured in the x and y-axis, likely causing an underestimation of migration rates. Cells displayed saltatory locomotion reminiscent of radial glial-guided migration, in which neurons extend a leading process and movement of the nucleus follows in a step-like fashion (Nadarajah et al., 2001). The saltatory motion was monitored throughout the migratory tracks of individual neurons (Figure 2C).

A population of fast-migrating neurons, which became more prevalent at P6/7, had an average migration speed of 49.3 μm/hr, with speeds ranging up to 105 μm/hr (Figure 2B and D). We suspected that the fast migrating cells were inhibitory interneurons migrating from the ventral forebrain, as in the rodent these cells have been shown to migrate substantially faster than pyramidal neurons (Ang et al., 2003; Valiente and Martini, 2009; Wichterle et al., 1999). Due to their speed, they migrated through the imaging field and we were unable to locate and assess marker expression post-time-lapse imaging. Therefore, in order to confirm that migrating interneurons were labeled by AAV2-CAG-GFP, the virus was applied to P6/7 slices that were then stained for the interneuron marker Lhx6. Indeed, GFP-positive cells expressing Lhx6 and displaying a leading process suggestive of migrating interneuron identity were present in the SVZ (Figure 2E).

Cortical plate-directed radial migration of ferret neurons decreases with age

In the rodent, it is thought that newborn projection neurons assume a bipolar morphology and migrate radially along one or more radial glia (RG) fibers to reach the cortical plate (CP) (Noctor et al., 2001; Rakic, 1971, 1972). In contrast, studies in the gyrencephalic cortex suggest that pyramidal neurons do not follow strict radial pathways and instead can disperse and migrate tangentially (Kornack and Rakic, 1995; O'Rourke et al., 1997; O'Rourke et al., 1992; Reid et al., 1997; Ware et al., 1999). In order to test this hypothesis, we assessed the directionality of migrating neurons in the developing ferret cortex.

Fast migrating neurons, determined as outliers using the ROUT method (Q = 1%) (Motulsky and Brown, 2006), were excluded from the analysis (5 cells from P2/3 and 45 cells from P6/7). For an imaging field, the displacement of each track along the x and y-axis was plotted according to time. Examples of displacement graphs from an imaging field at P2/3 (Figure 3A) and P6/7 (Figure 3B) are shown. A clear difference in the tracks can be seen. Specifically, the majority of migration tracks at P2/3 were in the direction of the cortical plate, whereas the directions of P6/7 migration tracks were more varied. In order to measure this quantitatively, the angle of migration of each cell was calculated based on the x, y displacement values from the last track time-point. This angle was then adjusted so that the direction of the cortical plate was between 45-135° for each imaging field. While the mean angle of the direction of migration was not significantly different between P2/3 and P6/7, the distribution of angles was significantly different ($p = 4.1 \times 10^{-7}$). The frequency of cells migrating in directions away from the CP was greater at P6/7 compared to P2/3. This difference was more pronounced for neurons migrating through the germinal zones (VZ and SVZ) ($p = 8.6 \times 10^{-8}$) than those migrating through the IZ and CP ($p = 0.02$) (Figure 3C and D).

These data suggest that at earlier stages of ferret cortical development, when the cortex is not yet folded, the majority of pyramidal neurons migrate radially into the CP, similar to what has been described in the rodent. However, at later ages when the cortex has begun to fold, pyramidal neurons do not follow strict radial pathways and instead can be observed migrating towards the VZ surface as well as tangentially, specifically when traversing the germinal zones.

Neuronal migration routes become more tortuous at later ages

In addition to an increase in the frequency of non-CP directed migration, neurons exhibited more frequent turns along their migratory pathways at later ages. We quantified this feature using a straightness index. Straightness was defined as the ratio of the distance between the first and last positions of a track and the actual length of the track (Figure 4D). The lower the straightness value, the more convoluted the migration path.

Again, fast migrating neurons were excluded from the analysis. We found that the straightness index was significantly decreased at P6/7 compared to P2/3 (Figure 4A). When average straightness was compared between regions, this age-related decrease was specific to neurons migrating within germinal regions (VZ and SVZ) (Figure 4B). This data suggests that ferret neurons migrating through the VZ and SVZ meander more along their paths at later ages. An example of a P6/7 neuron migrating within the SVZ and exhibiting several directional turns is shown in Figure 4C. The leading process is highly dynamic and prior to each turn appears to retract and then extend in a new direction before the nucleus begins to move. Similar properties of the leading process have been described in migrating interneurons in the rodent (Valiente and Martini, 2009).

Ferret neurons can migrate promiscuously along different radial glia fibers

The observations that P6/7 ferret neurons migrate in non-radial directions and change directions along their paths suggest that pyramidal neurons migrate along several different RG fibers while making their way to the CP. In order to test this, we labeled P6/7 RGs and their fibers with a CMV-tdtom plasmid. We then made cortical slices and labeled migrating neurons with AAV2-CAG-GFP (Figure 5A). Figure 5B shows an example of a GFP-positive neuron migrating towards the CP along a tdtom-positive RG fiber. After 16 hours of imaging, the leading process is observed to retract and extend towards the VZ along a neighboring RG fiber that is approximately 50 μm away. The nucleus then moves in the direction of the leading process and migrates along the neighboring fiber. The leading process subsequently extends along another nearby fiber with the soma eventually following. The neuron then ceases migration and the leading process extends towards the CP along the RG fiber along which it had previously been migrating. A schematic of the migration path and the RG fibers along which the neuron migrated are shown in Figure 5C.

In this example, the neuron makes two 180° directional turns, each of which is preceded by re-orientation of the leading process, which contacts and adheres to a different, nearby RG fiber. This data suggests that ferret neurons that meander along their path and make directional turns do so by migrating along several different RG fibers.

Divisions by AAV2-CAG-GFP labeled progenitors are neurogenic

While the majority of AAV2-CAG-GFP-positive cells displayed migratory behaviors and did not undergo mitosis, we observed a few GFP-positive cells that underwent divisions. An example of this is shown in Figure 6B, in which a GFP-positive cell rounded up and divided. This mitotic behavior is reminiscent of IPC divisions in the rodent (Noctor et al., 2004) and human (Hansen et al., 2010) and differs from the interkinetic nuclear migration of ventricular RGs (Miyata et al., 2001; Noctor et al., 2001) or the mitotic somal translocation of outer RGs (oRGs) (Gertz et al., 2014; Hansen et al., 2010; Ostrem et al., 2014; Wang et al., 2011). Because most AAV2-CAG-GFP-positive cells appear to be post-mitotic migrating neurons, we presumed that GFP-positive dividing cells were generating neurons. However, they could potentially be producing glial cells. Post-time-lapse fate staining revealed that daughters of AAV2-CAG-GFP-positive divisions at P2/3 expressed Sox2 but not Olig2, suggesting that they were not oligodendrocytes or oligodendrocyte precursor cells.

In order to further characterize these dividing cells, progenitor cells were labeled with both AV-CMV-mcherry, an adenovirus where mcherry expression is under control of the CMV promoter, and AAV2-CAG-GFP. We observed cells that started off expressing only mcherry until just before mitosis, when a GFP signal could be detected. Daughter cells from these divisions continued to express GFP, with signal intensity increasing over time. An example of this is shown in Figure 6A, with post-time-lapse fate staining revealing that daughters lacked Satb2 expression (data not shown), but expressed Sox2 and Tbr2, suggestive of IPC identity. These data suggest that AAV2-CAG-GFP-positive cell divisions are neurogenic and may produce cells that become pyramidal neurons.

Discussion

While recent advances have been made in classifying progenitor behaviors in gyrencephalic species (Betizeau et al., 2013; Gertz et al., 2014; Hansen et al., 2010; LaMonica et al., 2013; Ostrem et al., 2014), still little remains known about neuronal production and migration in the gyrencephalic cortex. In this study, we identified a method for visualizing neurogenic divisions and neuronal migration in the developing ferret, a carnivore with a gyrencephalic cortex, and performed a comprehensive analysis of neuronal migration. We observed a dramatic difference in the migration properties of neurons as a function of age, with non-radial, meandering migration more apparent at later ages. This was accompanied by neurons switching RG fibers along their migration path, revealing a mechanism by which neurons become tangentially dispersed in the gyrencephalic cortex. These properties are in contrast to the prevailing model of neuronal migration, primarily deduced from rodent studies, and may be a general feature of gyrencephalic cortical development.

We were able to visualize robust neuronal migration in the ferret by infecting cortical slices with an adeno-associated virus in which GFP expression is under the control of the CAG promoter (AAV2-CAG-GFP) (Figure 1). While AAV2-CAG-GFP labeled a substantial population of pyramidal neurons, infection of cortical slices with AV-CMV-GFP, an adenovirus in which GFP is expressed under the control of the CMV promoter, results in the labeling of very few migrating or mature neurons. Variations in cell infectivity or promoter expression may explain this difference. The viruses may infect different cell populations due to the difference in the viral backbones. Alternatively, they may infect similar populations, but GFP levels may vary due to differences in the promoter driving reporter expression. While CMV and CAG are constitutive promoters commonly used to drive reporter expression in mammalian tissue, differences in expression kinetics and cell-type specificity have been reported (Qin et al., 2010). For instance, the CMV promoter can become silenced in specific neuronal types (Gray et al., 2011). We observed CMV-mcherry-positive cells, which at a later time-point expressed CAG-GFP, suggesting that the viruses can infect similar cell populations and that promoter differences are responsible for variations in reporter expression (Figure 6A).

Time-lapse imaging of AAV2-CAG-GFP labeled slices revealed populations of slow and fast migrating neurons in the early postnatal ferret cortex. The vast majority of labeled cells had migration speeds between 4-20 μm/h and underwent saltatory migration, with periods of movement interspersed with pauses. These features are typical of excitatory neurons in the rodent (Nadarajah et al., 2001). Along with marker expression analysis (Figure 1), this suggests that slow migrating neurons were derived from the ferret dorsal cortex. Slow-migrating neurons exhibited either unipolar or bipolar morphology possessing a short, leading process. Neurons migrating with multipolar morphology, which has been described at early stages of neuronal migration in the rodent (Noctor et al., 2004; Tabata et al., 2009; Tabata and Nakajima, 2003), was not observed. Additionally, we did not find GFP-positive cells possessing a process extending to the pial surface or displaying somal translocation, a cell type described in the ferret (Borrell et al., 2006). It is possible that these morphologies are not adopted by ferret pyramidal neurons or that CAG-GFP is only detected in neurons with a short, leading process. Our data suggests that the smaller population of fast-migrating cells, which increased from 2% to 15% of the cells analyzed between P2/3 and P6/7, corresponds to inhibitory interneurons. Therefore, AAV2-CAG-GFP can be used to visualize the migration of both excitatory and inhibitory neurons in the developing ferret cortex.

At very early postnatal ages, the pattern of neuronal migration appeared nearly indistinguishable from the rodent. In general, neurons migrated radially towards the CP. However, just four days later, neurons displayed dramatically different migratory behaviors. Significantly more neurons migrated through the VZ and SVZ in non-radial directions, including towards the VZ as well as tangentially. Adding to the diversity in direction of migration, neurons at later ages meandered and frequently changed orientation, sometimes making 180° turns and re-tracing their paths. This data is consistent with the increased dispersion of clonally related neurons observed at later ages in the ferret (Reid et al., 1997; Ware et al., 1999). The dynamics of the leading process during directional changes is reminiscent of rodent interneurons (Valiente and Martini, 2009). Specifically, the leading process underwent repeated cycles of retraction, extension, and re-orientation and occasionally exhibited a branched morphology (data not shown) (Martini et al., 2009). However, migration speed and marker expression indicate that these cells are migrating pyramidal neurons. It appears that pyramidal neurons in the larger, folded cortex of the developing ferret behave more like interneurons in the rodent cortex, with the ability to migrate both radially and tangentially and possessing a dynamic leading process.

Changes in the radial fiber scaffold may account for neuronal migration differences during development of the ferret cortex. At P2, RG fibers in the SVZ appear parallel and predominantly radial. In contrast, P6 RG fibers in the SVZ undulate and are less radially aligned, while in the IZ and CP fibers are more radial (Reillo and Borrell, 2012). This could be due, in part, to the presence of oRG cells in the SVZ, that possess primary fibers that vary in orientation and are not always anchored to the pial surface (Gertz et al., 2014). Since cortical neurons use RG fibers as guides for migration, the increased disorganization of the fiber scaffold over time may cause neurons to display less radial and more dispersed migration at later ages. Interestingly, neuronal migration at P6 was less radial as neurons migrated through the VZ and SVZ and became more radial as cells migrated through the IZ and CP (Figure 3D), consistent with the patterning of the RG scaffold. Therefore, as previously proposed (Reillo et al., 2011), a divergent, fanned array of RG fibers may be responsible for the lateral dispersion of migrating ferret neurons within the SVZ. As a neuron approaches the IZ and CP, the increased parallel nature of the radial fiber scaffold may cause more radial-directed migration as a neuron navigates to the appropriate laminar position.

In addition to developmental changes in the radial fiber scaffold, the formation of gyri and sulci becomes apparent by P6 (Smart and McSherry, 1986a), when upper layer neurons are still being produced (Jackson et al., 1989; McConnell, 1988). In addition to residing in a specific cortical layer, neurons must decide which region of a gyrus or sulcus to occupy and disperse tangentially to populate the entire CP. This process may require neurons to integrate multiple extracellular cues, causing them to make more directional alterations at later ages.

The meandering and turning behaviors displayed by migrating ferret pyramidal neurons are inconsistent with the radial unit hypothesis. According to this model, neurons climb radially along one or more neighboring RG fibers, more often than not including the parent cell, so that a spatial map of the VZ is projected to the CP in a point-to-point manner (Rakic, 1988, 1995). Retroviral studies revealing the lateral dispersion of clonally related neurons in both the ferret (Reid et al., 1997; Ware et al., 1999) and primate (Kornack and Rakic, 1995) suggest that the model may not be strictly consistent with the development of the gyrencephalic cortex. Our real-time data provide further evidence that ferret pyramidal neurons do not follow a strict radial path to the CP, especially at later stages of neurogenesis. Specifically, we observed that neurons commonly switch the RG fiber along which they migrate, suggesting that ferret pyramidal neurons do not follow the trajectory of a single, parent RG fiber and instead migrate promiscuously along several different RG fibers. An observation consistent with this behavior was made based on electron microscopy images of the developing macaque cortex, where the leading process of a migrating neuron was noted to reach out and contact a neighboring RG fiber (Rakic et al., 1974). This pattern of migration likely promotes the tangential dispersion of pyramidal neurons in the developing gyrencephalic cortex (Lui et al., 2011).

The expression of AAV2-CAG-GFP appears to coincidence with commitment to the neuronal lineage, as most labeled cells are migrating neurons. However, we also observed GFP-positive cells that underwent IPC-like divisions. Because the daughter cells continued to express the IPC marker Tbr2 as well as GFP, it is likely that these are terminal divisions producing post-mitotic neurons. Cells in the developing ferret cortex may take longer to turn off Tbr2 expression, turn on Satb2 expression, and begin migrating compared to cells in the developing mouse cortex. The use of the AAV2-CAG-GFP labeling technique may be useful for visualizing lineage progression from a terminal, neurogenic division to a mature neuron within the CP.

Taken together, our data suggest that the horizontal dispersion of ferret pyramidal neurons during late neurogenesis is caused by the migration of neurons along a discontinuous path utilizing a diversity of radial glial scaffolds. These findings may be general to gyrencephalic species and support the use of non-rodent model systems for studying cellular dynamics that may be relevant to human neuronal migration disorders.

Figure 1. AAV2-CAG-GFP labels migrating neurons in the developing ferret cortex. (A) P2/3 cortical slice cultures were labeled with AV-CMV-GFP or AAV2-CAG-GFP and stained for Sox2, Tbr2, Olig2, or Satb2. Graph shows the mean percentage and SEM of GFP-positive cells expressing an individual marker. (B) Representative image of the OSVZ from a P2/3 slice labeled with AAV2-CAG-GFP and stained for Sox2 (blue) and Satb2 (red). White open arrowheads indicate GFP-positive cells expressing Satb2 and not Sox2, while yellow closed arrowheads indicate those expressing Sox2 and not Satb2. (C) Time-lapse stills of a migrating neuron labeled with AAV2-CAG-GFP in a P2/3 cortical slice (white arrowhead). Time elapsed from first frame in series indicated in top right of image (hr:min). VZ surface is down. Post time-lapse fate staining reveals that the GFP-positive cell is Satb2-positive and Sox2-negative. Scale bars = 20 μm.

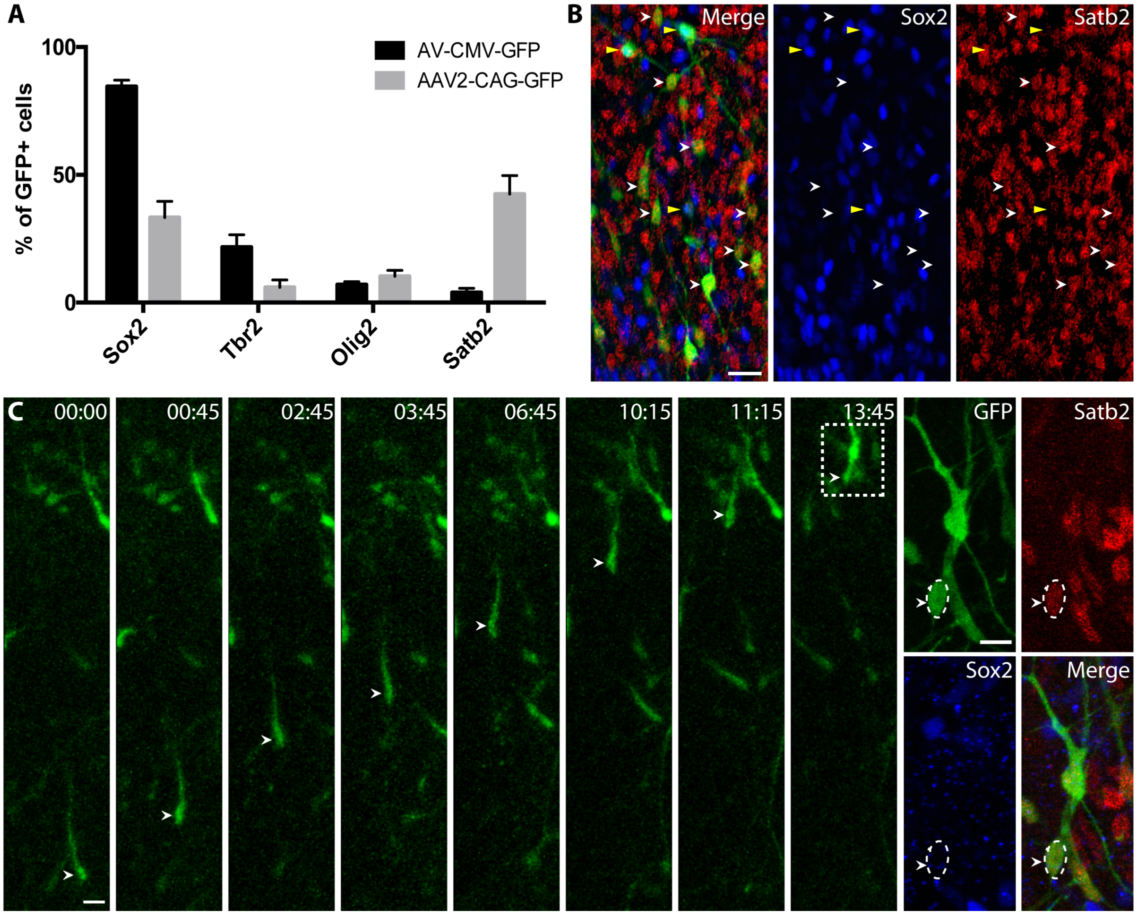
A
100
50
0
% of GFP+ cells
AV-CMV-GFP
AAV2-CAG-GFP
Sox2
Tbr2
Olig2
Satb2
B
Merge
Sox2
Satb2
C
00:00
00:45
02:45
03:45
06:45
10:15
11:15
13:45
GFP
Satb2
Sox2
Merge

Figure 2. Populations of fast and slow migrating cells can be detected in the ferret cortex.

(A) Example of an imaging field from a P2/3 ferret slice labeled with AAV2-CAG-GFP. VZ surface is down. Tracks generated in Imaris are shown with a time index. Scale bar = 100 μm. (B) Percentage of tracks within a specified mean track speed (μm/hr). A total of 277 and 302 tracks were analyzed at P2/3 and P6/7, respectively. (C) Example of three P2/3 migrating neurons that have an average track speed between 10-20 μm, with migration speed plotted over time. These cells exhibit saltatory migration. (D) Example of two P6/7 neurons that have an average track speed over 40 μm, with migration speed plotted over time. (E) P6/7 cortical slice labeled with AAV2-CAG-GFP and stained for Sox2 (blue) and the interneuron marker Lhx6 (gray). The arrowhead indicates a GFP-positive cell expressing both Sox2 and Lhx6 and possessing a leading process. Scale bar = 10 μm.

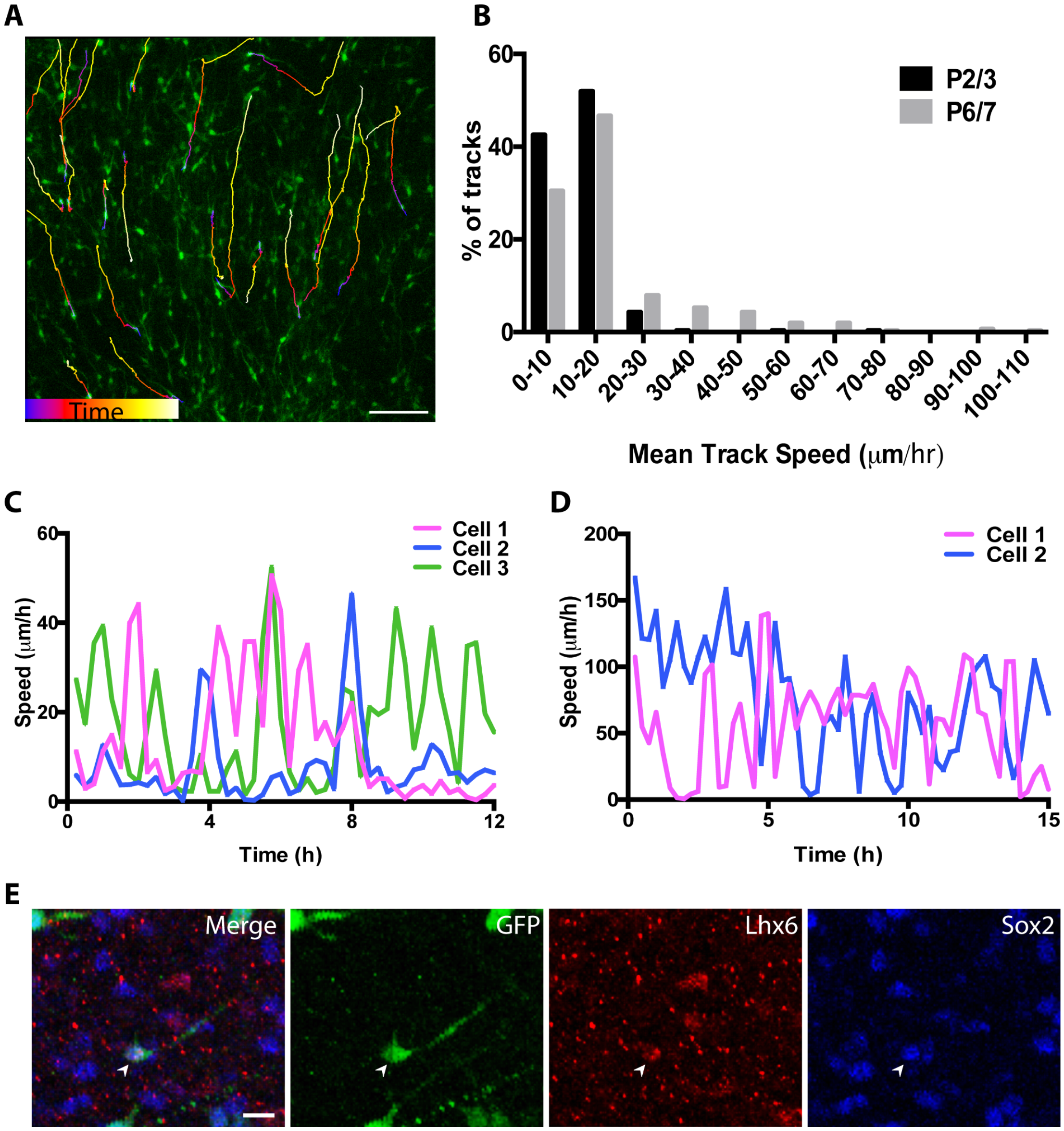
A
Time
B
60
40
20
0
% of tracks
P2/3
P6/7
0-10
10-20
20-30
30-40
40-50
50-60
60-70
70-80
80-90
90-100
100-110
Mean Track Speed (μm/hr)
C
Cell 1
Cell 2
Cell 3
60
40
20
0
Speed (μm/h)
0
4
8
12
Time (h)
D
Cell 1
Cell 2
200
150
100
50
0
Speed (μm/h)
0
5
10
15
Time (h)
E
Merge
GFP
Lhx6
Sox2

Figure 3. Cortical plate-directed radial migration of ferret neurons decreases with age. (A, B) Tracks generated from a single P2/3 imaging position in the VZ/SVZ (A) and a single P6/7 imaging position in the SVZ (B) plotted from a common origin (x=0, y=0) as displacement of x and y over time. The cortical plate is up (positive y values). (C, D) Rose plots of the direction of migration of P2/3 (C) and P6/7 (D) tracks from all imaged fields (minus fast migrating cells), only those from VZ/SVZ imaging fields, and only those from IZ/CP imaging fields (left to right). Each wedge represents a 20° interval with the frequency depicted by the radius length. The direction of the cortical plate is 45° to 135°, with 0° to the right. The red arrow indicates the vector sum (r), or the weighted average of migration direction.

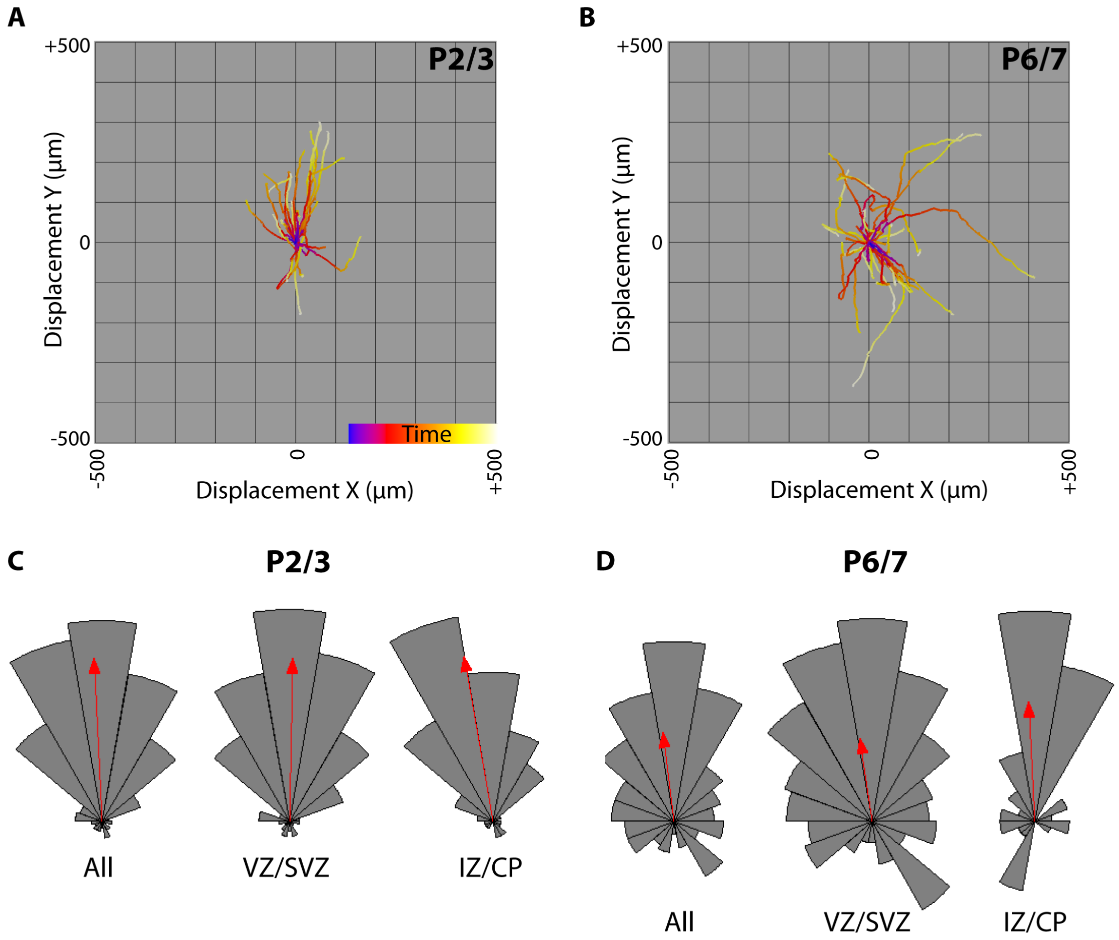
A
+500
P2/3
Displacement Y (µm)
0
-500
Time
-500
0
+500
Displacement X (µm)
B
+500
P6/7
Displacement Y (µm)
0
-500
-500
0
+500
Displacement X (µm)
C
P2/3
All
VZ/SVZ
IZ/CP
D
P6/7
All
VZ/SVZ
IZ/CP

Figure 4. Straightness of neuronal migration decreases with age.

(A) Box plot, showing min and max, of the straightness index of all tracks (minus fast migrating cells) at P2/3 and P6/7. Mean straightness of neuronal migratory tracks is significantly decreased at P6/7 compared to P2/3. (B) Average straightness of migrating neurons by age and region within the cortex. Straightness of migrating neurons is specifically decreased in the germinal zones (VZ/SVZ) at P6/7. (C) Time- lapse stills of an AAV2-CAG-GFP-labelled P6/P7 neuron in the OSVZ (white arrowhead) turning directions multiple times during imaging. Directional turns were preceded by re-orientation of the leading process (closed red arrowheads). Time elapsed from first frame in series indicated in top right of image (hr:min). VZ surface is down. Scale bars = 10 μm. (D) Schematic of the migration track of the neuron shown in (C) (black line). Straightness index of a track is determined by dividing the actual track length (black line, X) by the distance between the first and last points of the track (red dotted line, Y), which in this example equals 0.21. ****$p<0.0001$, ***$p<0.001$.

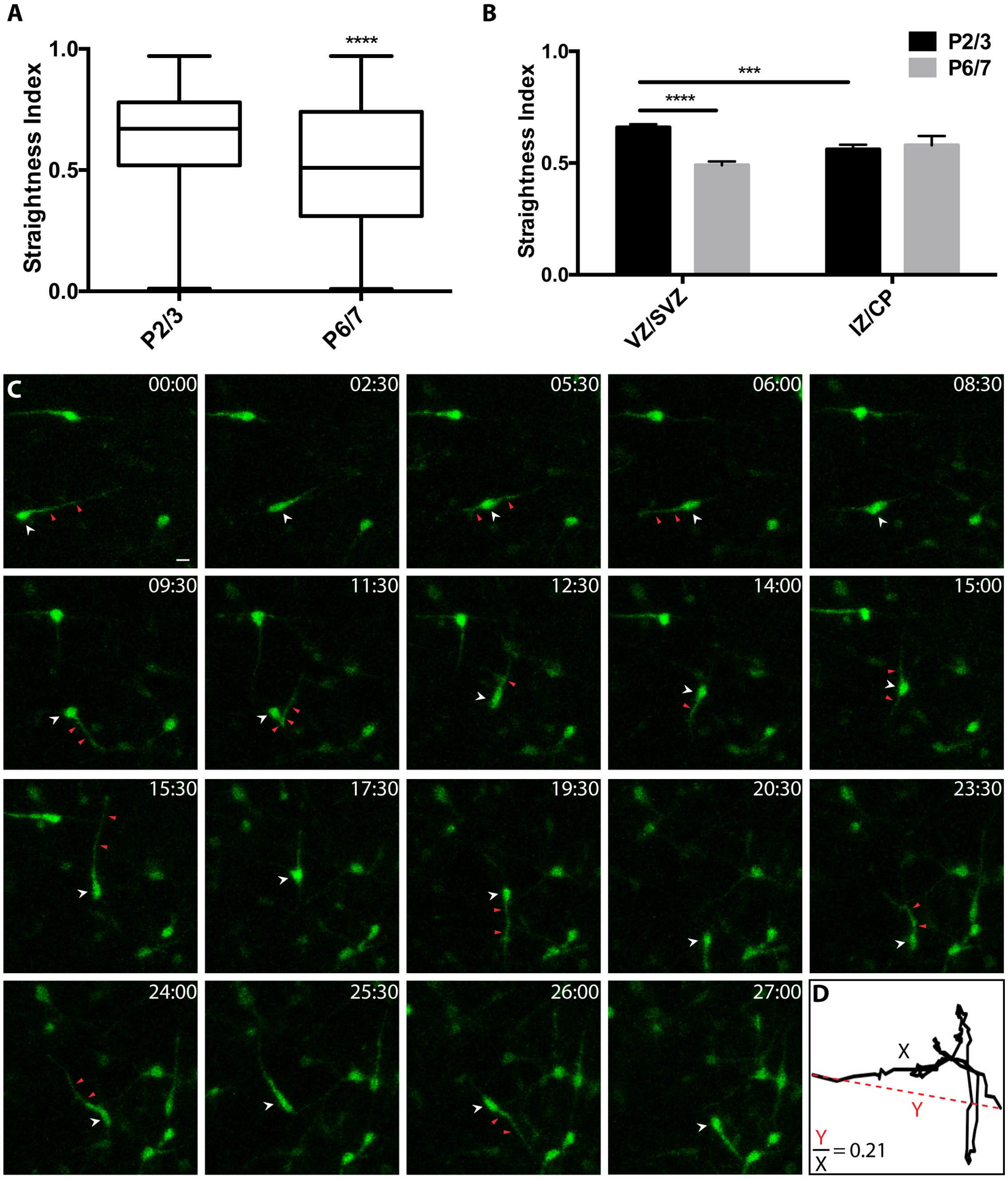
A
Straightness Index
1.0
0.5
0.0
****
P2/3
P6/7
B
Straightness Index
1.0
0.5
0.0
***
****
P2/3
P6/7
VZ/SVZ
IZ/CP
C
00:00
02:30
05:30
06:00
08:30
09:30
11:30
12:30
14:00
15:00
15:30
17:30
19:30
20:30
23:30
24:00
25:30
26:00
27:00
D
X
Y
Y/X = 0.21

Figure 5. Ferret neurons can migrate promiscuously along different radial glial fibers. (A) Schematic of experimental design. CMV-tdtom DNA was introduced into P7 ventricular radial glia in the lateral cortex by *ex utero* microinjection into the ventricle followed by electroporation. Coronal vibratome sections were then made and AAV2-CAG-GFP applied to sections via micropipette. (B) Time-lapse stills of a GFP-positive neuron in the SVZ (white open arrowhead) migrating along tdtom+ radial glia fibers. Directional turns were preceded by re-orientation of the leading process (closed light blue arrowheads). Time elapsed from first frame in series indicated in top right of image (hr:min). VZ surface is down. Scale bar = 20 μm. (C) Migration track of the neuron shown in B with a time index. Gray dotted lines indicate tdtom+ radial glial fibers.

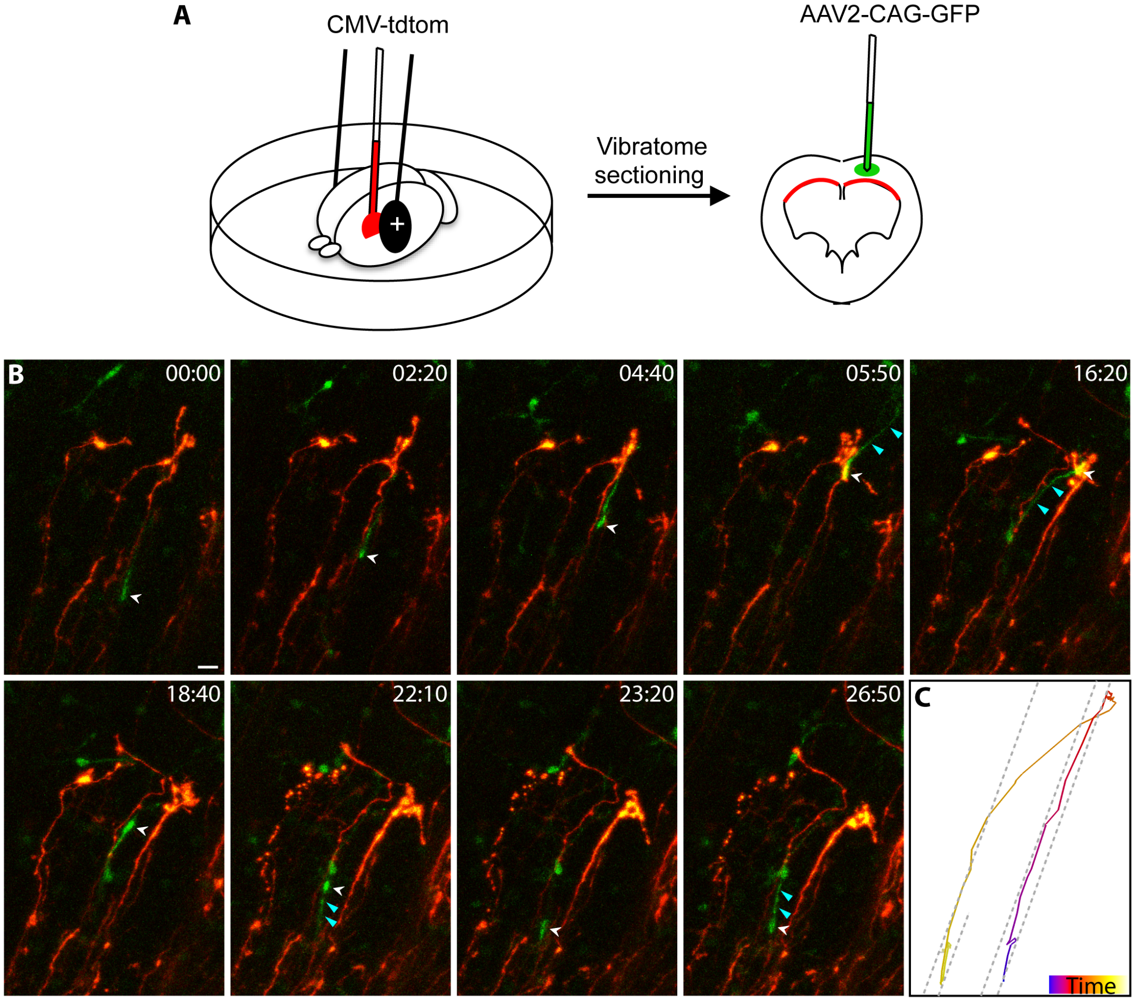
A
CMV-tdtom
Vibratome
sectioning
AAV2-CAG-GFP
B
00:00
02:20
04:40
05:50
16:20
18:40
22:10
23:20
26:50
C
Time

Figure 6. AAV2-CAG-GFP-positive cell divisions are IPC-like.

(A) AV-CMV-mcherry and AAV2-CAG-GFP viruses were mixed and applied to P2/3 ferret slices by micropipette. Time-lapse stills of a mcherry-positive cell that starts to become GFP-positive prior to mitosis and the production of two daughter cells (white arrowheads). Post time-lapse fate staining reveals that the GFP and mcherry-positive daughters express both Sox2 and Tbr2. (B) Time-lapse stills of a P2/3 AAV2-CAG-GFP labeled cell that undergoes a stationary division to produce daughters that are Sox2-positive and Olig2-negative (white arrowheads). (A, B) Time elapsed from first frame in series indicated in top right of image (hr:min), with start of division indicated in yellow. VZ surface is down. Scale bar = 10 μm.

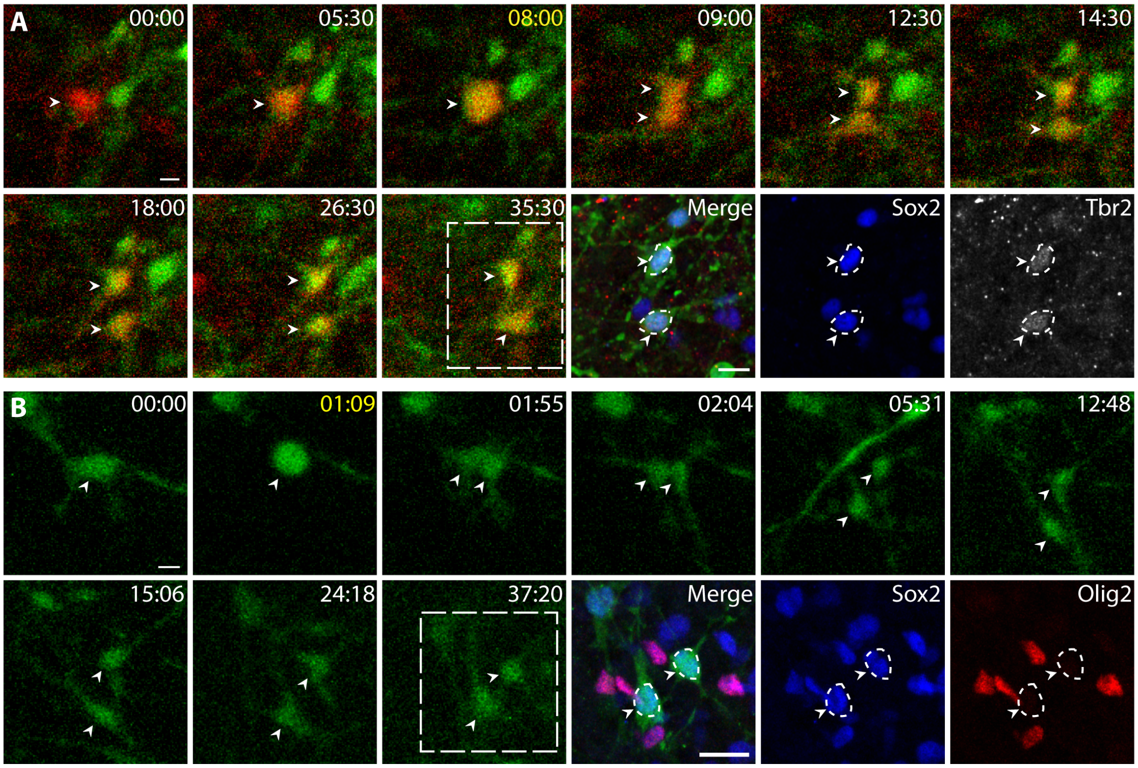
A
00:00
05:30
08:00
09:00
12:30
14:30
18:00
26:30
35:30
Merge
Sox2
Tbr2
B
00:00
01:09
01:55
02:04
05:31
12:48
15:06
24:18
37:20
Merge
Sox2
Olig2

CHAPTER 5:

General Conclusions

Over the past three decades, several models have been proposed regarding the cellular mechanisms underlying the evolutionary expansion and folding of the mammalian cerebral cortex. Recent hypotheses have focused on the role of the subventricular zone (SVZ) and the neural progenitors residing within this region during cortical development. Specifically, the identification and characterization of outer radial glia (oRG) within the last five years has led to current theories of cortical evolution, which propose that an increase in oRG generation and a subsequent increase in neuronal production led to an expanded and folded cortex (Lui et al., 2011). Despite an increased abundance of oRGs in the gyrencephalic primate compared to the lissencephalic rodent, the relative number of oRGs alone does not appear to predict adult cortical topography (Hevner and Haydar, 2012). It is likely that cell cycle dynamics and daughter cell fates determine the contribution of oRGs to cortical development. Other neural progenitor populations in the SVZ, such as intermediate progenitor cells (IPCs), may also play a role in shaping the adult cortex (Kriegstein et al., 2006). Moreover, as defects in neuronal migration underlie the development of neurodevelopmental diseases such as lissencephaly, a disorder in which patients lack gyri and sulci, neuronal migration properties may also regulate the development of gyrencephaly (Ross and Walsh, 2001).

In order to dissect the role of specific cell populations, such as oRGs, IPCs, or neurons, in cortical expansion and folding, an appropriate animal model is needed. Similar to humans, the ferret is gyrencephalic and possesses an expanded SVZ with abundant oRGs (Fietz et al., 2010; Reillo and Borrell, 2012; Reillo et al., 2011). However, unlike humans, it is experimentally tractable in that virus and plasmid DNA can be delivered both embryonically and postnatally and analyses performed in the adult. In order to establish the ferret as a model system to study cortical expansion and folding, I analyzed the behaviors of progenitors and neurons using time-lapse imaging. Observing cellular dynamics in real-time is a powerful technique that has yielded valuable insights into cortical development. These discoveries would not have been possible with the use of static analyses alone.

I demonstrate that similar to marker expression analyses, the ferret SVZ contains an abundance of oRGs with many undergoing mitotic somal translocation, a unique mode of division that was first identified in human oRGs (Hansen et al., 2010). However, unlike the human, a subset of ferret oRGs does not exhibit MST and instead undergoes stationary divisions. It will be interesting to determine whether different molecular mechanisms control MST versus stationary divisions of oRGs. I go on to show that ferret oRGs are more likely to undergo symmetric, self-renewing divisions and are less likely to produce IPC daughters compared to what has been observed in the human (Hansen et al., 2010). This difference in daughter cell fates suggests that oRGs in the human contribute more to neurogenesis. I also demonstrate diversity within the ferret and human oRG populations in terms of morphology, division mode, and location. Single-cell sequencing experiments are currently underway to determine whether this behavioral diversity is accompanied by molecular diversity within the progenitor population. Differences in oRG behaviors between the ferret and human, as well as diversity within the oRG population, are important features that must be taken into account when using the ferret to study cortical expansion and folding.

During development of a smooth versus folded cortex, several cellular and morphological differences exist that may cause variations in the dynamics of pyramidal neuron migration. For instance, due to the expanded SVZ size in gyrencephalic species, neurons must migrate longer distances to reach the appropriate cortical layer. In addition, a higher abundance of oRGs, whose fibers presumably support neuronal migration, as well as the formation of gyri and sulci while neurons are still migrating to their final destinations, adds increased complexity to the migratory pathways in a folded cortex. However, neuronal migration has not been extensively studied in gyrencephalic species. I first identified a technique to visualize both neurogenic divisions and neuronal migration in the ferret cortex. I show that similar to the rodent (Evsyukova et al., 2013), pyramidal neurons migrate radially towards the cortical plate at early stages of ferret development when the brain is not yet folded. In contrast, neurons exhibit more varied directions of migration and increased meandering at later ages when the cortex has begun to fold. I show that the tortuous migration pathways at later ages are accompanied by neurons migrating along several different radial glia fibers, which is the first demonstration of this behavior in real-time. These data suggest that later in neurogenesis, pyramidal neurons disperse tangentially by migrating sequentially along different radial glial fibers. It will be interesting to determine whether neuronal migration properties differ between cells destined for a developing gyrus or sulcus. These results challenge the longstanding model regarding pyramidal neuron migration, in which neurons follow strict radial pathways to the cortex. Additionally, it provides the first comprehensive analysis of the migration dynamics of pyramidal neurons in a folded cortex. It will be interesting to determine whether these behaviors are general to gyrencephalic species and if they are important for the proper development of cortical folds.

My graduate work highlights similarities and differences between ferret and primate cortical development and provides a framework for the future use of the ferret to study cellular and molecular mechanisms of cortical expansion and folding. It will be interesting to determine how genetic manipulations that alter the proliferative capacity of specific progenitor populations, such as IPCs or oRGs, effects the size and shape of the adult ferret cortex. It will also be exciting to model neuronal migration disorders, such as lissencephaly, in the ferret, as these diseases have proven difficult to model in the rodent. I hope that the implementation of the ferret as a model system will shed light on mechanisms underlying the evolution of the primate cortex, as well as human neurodevelopmental diseases.

References

Alvarez-Buylla, A., Theelen, M., and Nottebohm, F. (1988). Mapping of radial glia and of a new cell type in adult canary brain. The Journal of neuroscience : the official journal of the Society for Neuroscience *8*, 2707-2712.

Alvarez-Buylla, A., Theelen, M., and Nottebohm, F. (1990). Proliferation "hot spots" in adult avian ventricular zone reveal radial cell division. Neuron *5*, 101-109.

Ang, E.S., Jr., Haydar, T.F., Gluncic, V., and Rakic, P. (2003). Four-dimensional migratory coordinates of GABAergic interneurons in the developing mouse cortex. The Journal of neuroscience : the official journal of the Society for Neuroscience *23*, 5805-5815.

Angevine, J.B., Jr., and Sidman, R.L. (1961). Autoradiographic study of cell migration during histogenesis of cerebral cortex in the mouse. Nature *192*, 766-768.

Ayala, R., Shu, T., and Tsai, L.H. (2007). Trekking across the brain: the journey of neuronal migration. Cell *128*, 29-43.

Bayatti, N., Moss, J.A., Sun, L., Ambrose, P., Ward, J.F., Lindsay, S., and Clowry, G.J. (2008). A molecular neuroanatomical study of the developing human neocortex from 8 to 17 postconceptional weeks revealing the early differentiation of the subplate and subventricular zone. Cerebral cortex *18*, 1536-1548.

Bentivoglio, M., and Mazzarello, P. (1999). The history of radial glia. Brain research bulletin *49*, 305-315.

Betizeau, M., Cortay, V., Patti, D., Pfister, S., Gautier, E., Bellemin-Menard, A., Afanassieff, M., Huissoud, C., Douglas, R.J., Kennedy, H., *et al.* (2013). Precursor diversity and complexity of lineage relationships in the outer subventricular zone of the primate. Neuron *80*, 442-457.

Borrell, V. (2010). In vivo gene delivery to the postnatal ferret cerebral cortex by DNA electroporation. Journal of neuroscience methods *186*, 186-195.

Borrell, V., Kaspar, B.K., Gage, F.H., and Callaway, E.M. (2006). In vivo evidence for radial migration of neurons by long-distance somal translocation in the developing ferret visual cortex. Cerebral cortex *16*, 1571-1583.

Borrell, V., and Reillo, I. (2012). Emerging roles of neural stem cells in cerebral cortex development and evolution. Developmental neurobiology *72*, 955-971.

Chenn, A., and McConnell, S.K. (1995). Cleavage orientation and the asymmetric inheritance of Notch1 immunoreactivity in mammalian neurogenesis. Cell *82*, 631-641.

Chenn, A., and Walsh, C.A. (2002). Regulation of cerebral cortical size by control of cell cycle exit in neural precursors. Science *297*, 365-369.

Chenn, A., and Walsh, C.A. (2003). Increased neuronal production, enlarged forebrains and cytoarchitectural distortions in beta-catenin overexpressing transgenic mice. Cerebral cortex *13*, 599-606.

Dehay, C., and Kennedy, H. (2007). Cell-cycle control and cortical development. Nature reviews Neuroscience *8*, 438-450.

Edmondson, J.C., and Hatten, M.E. (1987). Glial-guided granule neuron migration in vitro: a high-resolution time-lapse video microscopic study. The Journal of neuroscience : the official journal of the Society for Neuroscience *7*, 1928-1934.

Englund, C., Fink, A., Lau, C., Pham, D., Daza, R.A., Bulfone, A., Kowalczyk, T., and Hevner, R.F. (2005). Pax6, Tbr2, and Tbr1 are expressed sequentially by radial glia, intermediate progenitor cells, and postmitotic neurons in developing neocortex. The Journal of neuroscience : the official journal of the Society for Neuroscience *25*, 247-251.

Evsyukova, I., Plestant, C., and Anton, E.S. (2013). Integrative mechanisms of oriented neuronal migration in the developing brain. Annual review of cell and developmental biology *29*, 299-353.

Fietz, S.A., Kelava, I., Vogt, J., Wilsch-Brauninger, M., Stenzel, D., Fish, J.L., Corbeil, D., Riehn, A., Distler, W., Nitsch, R., *et al.* (2010). OSVZ progenitors of human and ferret neocortex are epithelial-like and expand by integrin signaling. Nature neuroscience *13*, 690-699.

Fish, J.L., Dehay, C., Kennedy, H., and Huttner, W.B. (2008). Making bigger brains-the evolution of neural-progenitor-cell division. Journal of cell science *121*, 2783-2793.

Florio, M., and Huttner, W.B. (2014). Neural progenitors, neurogenesis and the evolution of the neocortex. Development *141*, 2182-2194.

Garcia-Moreno, F., Vasistha, N.A., Trevia, N., Bourne, J.A., and Molnar, Z. (2012). Compartmentalization of cerebral cortical germinal zones in a lissencephalic primate and gyrencephalic rodent. Cerebral cortex *22*, 482-492.

Gertz, C.C., Lui, J.H., LaMonica, B.E., Wang, X., and Kriegstein, A.R. (2014). Diverse behaviors of outer radial glia in developing ferret and human cortex. The Journal of neuroscience : the official journal of the Society for Neuroscience *34*, 2559-2570.

Gray, S.J., Foti, S.B., Schwartz, J.W., Bachaboina, L., Taylor-Blake, B., Coleman, J., Ehlers, M.D., Zylka, M.J., McCown, T.J., and Samulski, R.J. (2011). Optimizing promoters for recombinant adeno-associated virus-mediated gene expression in the peripheral and central nervous system using self-complementary vectors. Human gene therapy *22*, 1143-1153.

Hansen, D.V., Lui, J.H., Parker, P.R., and Kriegstein, A.R. (2010). Neurogenic radial glia in the outer subventricular zone of human neocortex. Nature *464*, 554-561.

Haubensak, W., Attardo, A., Denk, W., and Huttner, W.B. (2004). Neurons arise in the basal neuroepithelium of the early mammalian telencephalon: a major site of neurogenesis. Proceedings of the National Academy of Sciences of the United States of America *101*, 3196-3201.

Haubst, N., Georges-Labouesse, E., De Arcangelis, A., Mayer, U., and Gotz, M. (2006). Basement membrane attachment is dispensable for radial glial cell fate and for proliferation, but affects positioning of neuronal subtypes. Development *133*, 3245-3254.

Haydar, T.F., Kuan, C.Y., Flavell, R.A., and Rakic, P. (1999). The role of cell death in regulating the size and shape of the mammalian forebrain. Cerebral cortex *9*, 621-626.

Hevner, R.F., and Haydar, T.F. (2012). The (not necessarily) convoluted role of basal radial glia in cortical neurogenesis. Cerebral cortex *22*, 465-468.

Hofman, M.A. (2014). Evolution of the human brain: when bigger is better. Frontiers in neuroanatomy *8*, 15.

Jackson, C.A., Peduzzi, J.D., and Hickey, T.L. (1989). Visual cortex development in the ferret. I. Genesis and migration of visual cortical neurons. The Journal of neuroscience : the official journal of the Society for Neuroscience *9*, 1242-1253.

Kawasaki, H., Toda, T., and Tanno, K. (2013). In vivo genetic manipulation of cortical progenitors in gyrencephalic carnivores using in utero electroporation. Biology open *2*, 95-100.

Kelava, I., Reillo, I., Murayama, A.Y., Kalinka, A.T., Stenzel, D., Tomancak, P., Matsuzaki, F., Lebrand, C., Sasaki, E., Schwamborn, J.C., *et al.* (2012). Abundant occurrence of basal radial glia in the subventricular zone of embryonic neocortex of a lissencephalic primate, the common marmoset Callithrix jacchus. Cerebral cortex *22*, 469-481.

Kornack, D.R., and Rakic, P. (1995). Radial and horizontal deployment of clonally related cells in the primate neocortex: relationship to distinct mitotic lineages. Neuron *15*, 311-321.

Kriegstein, A., Noctor, S., and Martinez-Cerdeno, V. (2006). Patterns of neural stem and progenitor cell division may underlie evolutionary cortical expansion. Nature reviews Neuroscience *7*, 883-890.

Kuida, K., Zheng, T.S., Na, S., Kuan, C., Yang, D., Karasuyama, H., Rakic, P., and Flavell, R.A. (1996). Decreased apoptosis in the brain and premature lethality in CPP32-deficient mice. Nature *384*, 368-372.

LaMonica, B.E., Lui, J.H., Hansen, D.V., and Kriegstein, A.R. (2013). Mitotic spindle orientation predicts outer radial glial cell generation in human neocortex. Nature communications *4*, 1665.

Levitt, P., Cooper, M.L., and Rakic, P. (1981). Coexistence of neuronal and glial precursor cells in the cerebral ventricular zone of the fetal monkey: an ultrastructural immunoperoxidase analysis. The Journal of neuroscience : the official journal of the Society for Neuroscience *1*, 27-39.

Lewitus, E., Kelava, I., and Huttner, W.B. (2013). Conical expansion of the outer subventricular zone and the role of neocortical folding in evolution and development. Frontiers in human neuroscience *7*, 424.

Lui, J.H., Hansen, D.V., and Kriegstein, A.R. (2011). Development and evolution of the human neocortex. Cell *146*, 18-36.

Lukaszewicz, A., Savatier, P., Cortay, V., Giroud, P., Huissoud, C., Berland, M., Kennedy, H., and Dehay, C. (2005). G1 phase regulation, area-specific cell cycle control, and cytoarchitectonics in the primate cortex. Neuron *47*, 353-364.

Luskin, M.B., and Shatz, C.J. (1985). Neurogenesis of the cat's primary visual cortex. The Journal of comparative neurology *242*, 611-631.

Malatesta, P., Hartfuss, E., and Gotz, M. (2000). Isolation of radial glial cells by fluorescent-activated cell sorting reveals a neuronal lineage. Development *127*, 5253-5263.

Marin, O., and Rubenstein, J.L. (2001). A long, remarkable journey: tangential migration in the telencephalon. Nature reviews Neuroscience *2*, 780-790.

Marin, O., and Rubenstein, J.L. (2003). Cell migration in the forebrain. Annual review of neuroscience *26*, 441-483.

Marin, O., Valiente, M., Ge, X., and Tsai, L.H. (2010). Guiding neuronal cell migrations. Cold Spring Harbor perspectives in biology *2*, a001834.

Martinez-Cerdeno, V., Cunningham, C.L., Camacho, J., Antczak, J.L., Prakash, A.N., Cziep, M.E., Walker, A.I., and Noctor, S.C. (2012). Comparative analysis of the subventricular zone in rat, ferret and macaque: evidence for an outer subventricular zone in rodents. PloS one *7*, e30178.

Martini, F.J., Valiente, M., Lopez Bendito, G., Szabo, G., Moya, F., Valdeolmillos, M., and Marin, O. (2009). Biased selection of leading process branches mediates chemotaxis during tangential neuronal migration. Development *136*, 41-50.

McConnell, S.K. (1988). Fates of visual cortical neurons in the ferret after isochronic and heterochronic transplantation. The Journal of neuroscience : the official journal of the Society for Neuroscience *8*, 945-974.

Miyata, T., Kawaguchi, A., Okano, H., and Ogawa, M. (2001). Asymmetric inheritance of radial glial fibers by cortical neurons. Neuron *31*, 727-741.

Miyata, T., Kawaguchi, A., Saito, K., Kawano, M., Muto, T., and Ogawa, M. (2004). Asymmetric production of surface-dividing and non-surface-dividing cortical progenitor cells. Development *131*, 3133-3145.

Mo, Z., and Zecevic, N. (2008). Is Pax6 critical for neurogenesis in the human fetal brain? Cerebral cortex *18*, 1455-1465.

Molnar, Z. (2011). Evolution of cerebral cortical development. Brain, behavior and evolution *78*, 94-107.

Moody, K.D., Bowman, T.A., and Lang, C.M. (1985). Laboratory management of the ferret for biomedical research. Laboratory animal science *35*, 272-279.

Motulsky, H.J., and Brown, R.E. (2006). Detecting outliers when fitting data with nonlinear regression - a new method based on robust nonlinear regression and the false discovery rate. BMC bioinformatics *7*, 123.

Nadarajah, B., Brunstrom, J.E., Grutzendler, J., Wong, R.O., and Pearlman, A.L. (2001). Two modes of radial migration in early development of the cerebral cortex. Nature neuroscience *4*, 143-150.

Nadarajah, B., and Parnavelas, J.G. (2002). Modes of neuronal migration in the developing cerebral cortex. Nature reviews Neuroscience *3*, 423-432.

Noctor, S.C., Flint, A.C., Weissman, T.A., Dammerman, R.S., and Kriegstein, A.R. (2001). Neurons derived from radial glial cells establish radial units in neocortex. Nature *409*, 714-720.

Noctor, S.C., Flint, A.C., Weissman, T.A., Wong, W.S., Clinton, B.K., and Kriegstein, A.R. (2002). Dividing precursor cells of the embryonic cortical ventricular zone have morphological and molecular characteristics of radial glia. The Journal of neuroscience : the official journal of the Society for Neuroscience *22*, 3161-3173.

Noctor, S.C., Martinez-Cerdeno, V., Ivic, L., and Kriegstein, A.R. (2004). Cortical neurons arise in symmetric and asymmetric division zones and migrate through specific phases. Nature neuroscience *7*, 136-144.

Noctor, S.C., Martinez-Cerdeno, V., and Kriegstein, A.R. (2008). Distinct behaviors of neural stem and progenitor cells underlie cortical neurogenesis. The Journal of comparative neurology *508*, 28-44.

Nonaka-Kinoshita, M., Reillo, I., Artegiani, B., Martinez-Martinez, M.A., Nelson, M., Borrell, V., and Calegari, F. (2013). Regulation of cerebral cortex size and folding by expansion of basal progenitors. The EMBO journal *32*, 1817-1828.

O'Rourke, N.A., Chenn, A., and McConnell, S.K. (1997). Postmitotic neurons migrate tangentially in the cortical ventricular zone. Development *124*, 997-1005.

O'Rourke, N.A., Dailey, M.E., Smith, S.J., and McConnell, S.K. (1992). Diverse migratory pathways in the developing cerebral cortex. Science *258*, 299-302.

O'Rourke, N.A., Sullivan, D.P., Kaznowski, C.E., Jacobs, A.A., and McConnell, S.K. (1995). Tangential migration of neurons in the developing cerebral cortex. Development *121*, 2165-2176.

Ostrem, B.E., Lui, J.H., Gertz, C.C., and Kriegstein, A.R. (2014). Control of outer radial glial stem cell mitosis in the human brain. Cell reports *8*, 656-664.

Peng, X., Alfoldi, J., Gori, K., Eisfeld, A.J., Tyler, S.R., Tisoncik-Go, J., Brawand, D., Law, G.L., Skunca, N., Hatta, M., *et al.* (2014). The draft genome sequence of the ferret (Mustela putorius furo) facilitates study of human respiratory disease. Nature biotechnology.

Pilz, G.A., Shitamukai, A., Reillo, I., Pacary, E., Schwausch, J., Stahl, R., Ninkovic, J., Snippert, H.J., Clevers, H., Godinho, L., *et al.* (2013). Amplification of progenitors in the mammalian telencephalon includes a new radial glial cell type. Nature communications *4*, 2125.

Qin, J.Y., Zhang, L., Clift, K.L., Hulur, I., Xiang, A.P., Ren, B.Z., and Lahn, B.T. (2010). Systematic comparison of constitutive promoters and the doxycycline-inducible promoter. PloS one *5*, e10611.

Rakic, P. (1971). Guidance of neurons migrating to the fetal monkey neocortex. Brain research *33*, 471-476.

Rakic, P. (1972). Mode of cell migration to the superficial layers of fetal monkey neocortex. The Journal of comparative neurology *145*, 61-83.

Rakic, P. (1974). Neurons in rhesus monkey visual cortex: systematic relation between time of origin and eventual disposition. Science *183*, 425-427.

Rakic, P. (1988). Specification of cerebral cortical areas. Science *241*, 170-176.

Rakic, P. (1995). A small step for the cell, a giant leap for mankind: a hypothesis of neocortical expansion during evolution. Trends in neurosciences *18*, 383-388.

Rakic, P. (2003). Developmental and evolutionary adaptations of cortical radial glia. Cerebral cortex *13*, 541-549.

Rakic, P. (2009). Evolution of the neocortex: a perspective from developmental biology. Nature reviews Neuroscience *10*, 724-735.

Rakic, P., Stensas, L.J., Sayre, E., and Sidman, R.L. (1974). Computer-aided three-dimensional reconstruction and quantitative analysis of cells from serial electron microscopic montages of foetal monkey brain. Nature *250*, 31-34.

Reid, C.B., Tavazoie, S.F., and Walsh, C.A. (1997). Clonal dispersion and evidence for asymmetric cell division in ferret cortex. Development *124*, 2441-2450.

Reillo, I., and Borrell, V. (2012). Germinal zones in the developing cerebral cortex of ferret: ontogeny, cell cycle kinetics, and diversity of progenitors. Cerebral cortex *22*, 2039-2054.

Reillo, I., de Juan Romero, C., Garcia-Cabezas, M.A., and Borrell, V. (2011). A role for intermediate radial glia in the tangential expansion of the mammalian cerebral cortex. Cerebral cortex *21*, 1674-1694.

Ross, M.E., and Walsh, C.A. (2001). Human brain malformations and their lessons for neuronal migration. Annual review of neuroscience *24*, 1041-1070.

Roth, K.A., Kuan, C., Haydar, T.F., D'Sa-Eipper, C., Shindler, K.S., Zheng, T.S., Kuida, K., Flavell, R.A., and Rakic, P. (2000). Epistatic and independent functions of caspase-3 and Bcl-X(L) in developmental programmed cell death. Proceedings of the National Academy of Sciences of the United States of America *97*, 466-471.

Shitamukai, A., Konno, D., and Matsuzaki, F. (2011). Oblique radial glial divisions in the developing mouse neocortex induce self-renewing progenitors outside the germinal zone that resemble primate outer subventricular zone progenitors. The Journal of neuroscience : the official journal of the Society for Neuroscience *31*, 3683-3695.

Smart, I.H., Dehay, C., Giroud, P., Berland, M., and Kennedy, H. (2002). Unique morphological features of the proliferative zones and postmitotic compartments of the neural epithelium giving rise to striate and extrastriate cortex in the monkey. Cerebral cortex *12*, 37-53.

Smart, I.H., and McSherry, G.M. (1986a). Gyrus formation in the cerebral cortex in the ferret. I. Description of the external changes. Journal of anatomy *146*, 141-152.

Smart, I.H., and McSherry, G.M. (1986b). Gyrus formation in the cerebral cortex of the ferret. II. Description of the internal histological changes. Journal of anatomy *147*, 27-43.

Sun, X., Yan, Z., Liu, X., Olivier, A.K., and Engelhardt, J.F. (2014). Genetic Engineering in the Ferret. In Biology and Diseases of the Ferret (John Wiley & Sons, Inc.), pp. 665-683.

Tabata, H., Kanatani, S., and Nakajima, K. (2009). Differences of migratory behavior between direct progeny of apical progenitors and basal progenitors in the developing cerebral cortex. Cerebral cortex *19*, 2092-2105.

Tabata, H., and Nakajima, K. (2003). Multipolar migration: the third mode of radial neuronal migration in the developing cerebral cortex. The Journal of neuroscience : the official journal of the Society for Neuroscience *23*, 9996-10001.

Takahashi, T., Nowakowski, R.S., and Caviness, V.S., Jr. (1996). Interkinetic and migratory behavior of a cohort of neocortical neurons arising in the early embryonic murine cerebral wall. The Journal of neuroscience : the official journal of the Society for Neuroscience *16*, 5762-5776.

Valiente, M., and Martini, F.J. (2009). Migration of cortical interneurons relies on branched leading process dynamics. Cell adhesion & migration *3*, 278-280.

Vogt, D., Hunt, R.F., Mandal, S., Sandberg, M., Silberberg, S.N., Nagasawa, T., Yang, Z., Baraban, S.C., and Rubenstein, J.L. (2014). Lhx6 directly regulates Arx and CXCR7 to determine cortical interneuron fate and laminar position. Neuron *82*, 350-364.

Wang, X., Tsai, J.W., LaMonica, B., and Kriegstein, A.R. (2011). A new subtype of progenitor cell in the mouse embryonic neocortex. Nature neuroscience *14*, 555-561.

Ware, M.L., Tavazoie, S.F., Reid, C.B., and Walsh, C.A. (1999). Coexistence of widespread clones and large radial clones in early embryonic ferret cortex. Cerebral cortex *9*, 636-645.

Wichterle, H., Garcia-Verdugo, J.M., Herrera, D.G., and Alvarez-Buylla, A. (1999). Young neurons from medial ganglionic eminence disperse in adult and embryonic brain. Nature neuroscience *2*, 461-466.

Yokota, Y., Eom, T.Y., Stanco, A., Kim, W.Y., Rao, S., Snider, W.D., and Anton, E.S. (2010). Cdc42 and Gsk3 modulate the dynamics of radial glial growth, inter-radial glial interactions and polarity in the developing cerebral cortex. Development *137*, 4101-4110.

Zecevic, N., Chen, Y., and Filipovic, R. (2005). Contributions of cortical subventricular zone to the development of the human cerebral cortex. The Journal of comparative neurology *491*, 109-122.

Zilles, K., Palomero-Gallagher, N., and Amunts, K. (2013). Development of cortical folding during evolution and ontogeny. Trends in neurosciences *36*, 275-284.

Publishing Agreement

It is the policy of the University to encourage the distribution of all theses, dissertations, and manuscripts. Copies of all UCSF theses, dissertations, and manuscripts will be routed to the library via the Graduate Division. The library will make all theses, dissertations, and manuscripts accessible to the public and will preserve these to the best of their abilities, in perpetuity.

I hereby grant permission to the Graduate Division of the University of California, San Francisco to release copies of my thesis, dissertation, or manuscript to the Campus Library to provide access and preservation, in whole or in part, in perpetuity.

Author Signature

1/30/15

Date